Distribution Agreement

In presenting this thesis or dissertation as a partial fulfillment of the requirements for an advanced degree from Emory University, I hereby grant Emory University and its agents the non-exclusive license to archive, make accessible, and display my thesis or dissertation in whole or in part in all forms of media, now or hereafter known, including display on the world wide web. I understand that I may select some access restrictions as part of the online submission of this thesis or dissertation. I retain all ownership rights to the copyright of the thesis or dissertation. I also retain the right to use in future works (such as articles or books) all or part of this thesis or dissertation.

Signature:

_____ _____

Susan Margueritte Cox Date

Determining Greek Architectural Design Units in the Sanctuary of the Great Gods, Samothrace: Application of and Extensions to the Cosine Quantogram Method

By

Susan Margueritte Cox
Master of Science

Biostatistics

Vicki Stover Hertzberg, Ph.D.
Advisor

Brent A. Johnson, Ph.D.
Committee Member

Bonna D. Wescoat, D.Phil.
Committee Member

Accepted:

Lisa A. Tedesco, Ph.D.
Dean of the Graduate School

Date

Determining Greek Architectural Design Units in the Sanctuary of the Great Gods, Samothrace: Application of and Extensions to the Cosine Quantogram Method

By

Susan Margueritte Cox
B.S., Salem College, 2006

Advisor: Vicki Stover Hertzberg, Ph.D.

An abstract of
A thesis submitted to the Faculty of the Graduate School of Emory University
in partial fulfillment of the requirements for the degree of
Master of Science
in Biostatistics
2009

Abstract

Determining Greek Architectural Design Units in the Sanctuary of the Great Gods, Samothrace: Application of and Extensions to the Cosine Quantogram Method

By Susan Margueritte Cox

Investigations into derivations of ancient Greek architectural units of measure have been limited in their statistical rigor. The primary method to find an indivisible unit, the *quantum*, has been D. G. Kendall's cosine quantogram analysis (1974), used by J. Pakkanen (2002; 2004a; 2004b; 2005) to calculate quanta based on architectural components. However, no inference has been conducted beyond simple point estimation and testing a quantum's existence. We expand Kendall's method by calculating standard bootstrap confidence intervals for point estimates and introducing a likelihood ratio-based hypothesis test for the equality of quanta between buildings at the same site.

As a case study, individual block dimensions from two Doric structures are considered from the Sanctuary of the Great Gods, located on the island of Samothrace: the Dedication and the Hieron. The cosine quantogram method yielded a quantum of 0.211 m. for the Dedication (95% CI: (0.070 m., 0.352 m.)) and the quantum for the Hieron is 0.253 m. (95% CI: (0.163 m., 0.343 m.)). There is no statistically significant difference between these two quanta ($p = 0.270$), although in architectural terms, they differ considerably. The possibility of a 0.208-m. quantum, which indicates that the Dedication may have been designed based on the interaxial distance between columns due to a 1:10 ratio between the quantum and the interaxial space, is also explored. A 0.253-m. quantum indicates that the Hieron was probably designed with the outer dimensions in mind since the ratio between the quantum to the building's width and length at the level of the stylobate is 1:50:155. Future directions of this method are presented as well as potential applications to biology and public health.

Determining Greek Architectural Design Units in the Sanctuary of the Great Gods, Samothrace: Application of and Extensions to the Cosine Quantogram Method

By

Susan Margueritte Cox
B.S., Salem College, 2006

Advisor: Vicki Stover Hertzberg, Ph.D.

A thesis submitted to the Faculty of the Graduate School of Emory University
in partial fulfillment of the requirements for the degree of
Master of Science
in Biostatistics
2009

Acknowledgments

I would like to thank Drs. Vicki Hertzberg and Bonna Wescoat for making it possible for me to travel to Samothrace, Greece last summer to gain firsthand knowledge of Ancient Greek architecture and archaeology. Working at the site was an experience I will never forget. I also thank James R. McCredie, Director of the Excavations of Samothrace (NYU-IFA), and Dimitris Matsas, archaeologist of the 19th Ephorate of Prehistoric and Classical Antiquities (Komotini) for their encouragement of this project.

My advisor, Dr. Hertzberg, gave unselfishly of her time and expertise throughout this project. It was a pleasure working with her.

Dr. Wescoat helped me understand and interpret a vast amount of information concerning the island of Samothrace and its architecture. This thesis would not have been possible without her help.

I would also like to thank Dr. Brent Johnson. He not only served as my academic advisor prior to my thesis work, but was also an invaluable member of my thesis committee.

I am especially grateful for the support from my family and friends during the preparation of this thesis.

Contents

1 Introduction **1**

1.1 History of the Site and Excavations 1

1.2 The Study 3

1.3 Literature Review 5

2 Methods **9**

2.1 The Sample 9

2.2 Block Dimensions 11

2.3 Quantum Model 11

2.4 Calculations 12

2.4.1 Cosine Quantogram 12

2.4.2 Lower and Upper Bounds of q 13

2.4.3 Unrounding 13

2.5 Hypothesis Testing 15

2.5.1 Monte Carlo Simulations and Bootstrapping 19

2.6 Diagnostics 22

2.6.1 Conversion of Linear Data to Circular/Angular Data 22

2.6.2 Goodness-of-Fit Tests 22

2.6.3 Significance Testing for μ (κ Unknown) 23

2.6.4 Homogeneity between Pairs of Subsets 23

2.7 Software Packages 24

3 Results **25**

3.1 Missing Data 25

3.2 Univariate Analysis of Block Subgroups between Buildings 28

3.3 Comparison of Quanta between Buildings 30
3.4 Comparison of Quanta between Block Types within Buildings 36
3.4.1 Comparison of Quanta between Block Types of the Dedication 36
3.4.2 Comparison of Quanta between Block Types of the Hieron . . 41
3.5 Diagnostics 46
3.5.1 Goodness-of-Fit Tests 46
3.5.2 Significance Testing for the Mean Direction Parameter, μ . . . 46
3.5.3 Two-Sample Tests of Homogeneity 50

4 Discussion **51**
4.1 Art Historical Implications of the Calculated Quanta 51
4.2 Sources of Error in Block Dimensions 56
4.3 Limitations of Previous Studies 57
4.4 Limitations of This Study 58
4.5 Biological Applications 59
4.6 Public Health Implications 60
4.7 Future Directions 61

A Appendix: SAS Program for the Cosine Quantogram Method **64**

References **74**

List of Tables

1 Table of Cubits (Ordered from Largest to Smallest) 14

2 Table of Dactyls (Ordered from Largest to Smallest) 14

3 Probability of Rejecting H_0 in Monte Carlo Tests 21

4 Summary of Blocks Used 25

5 Summary of Block Measurements Used 26

6 Summary of Measurements of Subgroups of Blocks between Buildings 29

7 Comparison of Quanta between Buildings 30

8 Comparison of Quanta between Wall Blocks and Frieze Elements of the Dedication 36

9 Comparison of Quanta between Wall Blocks and Frieze Elements of the Hieron 41

10 Use of a 0.211-meter and a 0.208-meter Quantum in the Dedication . 52

11 Summary of Errors Produced with a 0.208-meter and a 0.211-meter Quantum in the Dedication 54

12 Use of a 0.253-meter Quantum in the Hieron 55

List of Figures

1 Histogram and KDE Function of Measurements from the Dedication and Hieron 31

2 Histogram and KDE Function of Measurements from the Dedication . 32

3 Histogram and KDE Function of Measurements from the Hieron . . . 33

4 Cosine Quantogram Plot for Wall Blocks and Frieze Elements from the Dedication 34

5 Cosine Quantogram Plot for Wall Blocks and Frieze Elements from the Hieron 35

6 Histogram and KDE Function of Wall Blocks Measurements from the Dedication 37

7 Histogram and KDE Function of Frieze Element Measurements from the Dedication 38

8 Cosine Quantogram Plot for Wall Blocks from the Dedication 39

9 Cosine Quantogram Plot for Frieze Elements from the Dedication . . 40

10 Histogram and KDE Function of Wall Block Measurements from the Hieron 42

11 Histogram and KDE Function of Frieze Element Measurements from the Hieron 43

12 Cosine Quantogram Plot for Wall Blocks from the Hieron 44

13 Cosine Quantogram Plot for Frieze Elements from the Hieron 45

14 Distribution of Calculated Errors Assuming a Von Mises Distribution for Measurements from the Dedication 48

15 Distribution of Calculated Errors Assuming a Von Mises Distribution for Measurements from the Hieron 49

1 Introduction

1.1 History of the Site and Excavations

The Sanctuary of the Great Gods is an archaeological site on the Greek island of Samothrace, located in the northeast Aegean Sea. Historically, the Sanctuary was a major seat of religious life during the late Classical period (beginning around the middle of the 4th century BCE) until the 3rd century CE. The distinguishing feature of this site was its association with a mystery cult whose rituals were known only to initiates of the cult. Initiation rites took place in the Sanctuary and there was no discrimination based on sex, age, or social status. Various important historical figures during the era wrote about, visited, or were initiated in the Sanctuary. Among these were Herodotus, the 'Father of History;' Lysander, the Spartan General; Marcus Terentius Varro, the Roman scholar; and L. Calpurnius Piso Caesoninus, consul of the Roman Republic and father-in-law of Julius Caesar. It was during their initiations that the Macedonian king Philip II met his fifth wife, Olympias, who later bore him Alexander the Great. Furthermore, Philip II and his successors became major patrons of the Sanctuary, causing the site to reach its zenith in the 3rd and 2nd centuries BCE (Matsas & Bakirtzis, 2001).

The Samothracian Mysteries centered on a pantheon of four gods, known as the Theoi Megaloi, or 'Great Gods.' They are also referred to as the Kabeiroi. Axieros, the Great Mother, was the principal goddess whose Greek counterpart was Demeter. Two other gods, Axiokersa and Axiokersos, are associated with Persephone and Hades, respectively. The fourth, Kadmilos, is equivalent to the Greek god Hermes. The local heroes of Samothrace, separate from the Great Gods, had their own associated rituals within the Sanctuary. Zeus and Elektra, daughter of Atlas, conceived Dardanos, Aetion, and Harmonia. Dardanos founded the Trojan race; Aetion taught

the mysteries to mortals. An annual festival included a dramatic interpretation of the wedding between Harmonia and the hero Kadmos, brother of Europa and founder of Thebes. This myth is similar to, and may have evolved from, the rape of Persephone by Hades and their subsequent marriage. Although the details of the Mysteries were never divulged, archaeological evidence suggests that animal sacrifices and libations were offered to the underworld gods (K. Lehmann, 1998).

Exploration of the site started in 1854 with the German archaeologists Ernst Otto Blau and Konstantin Schlottmann followed by Alexander Conze of Austria in 1858. In 1863 the French archaeologist Charles François Noël Champoiseau discovered the statue of the *Winged Victory of Samothrace* (ca. 200-190 BCE) and sent it back to Paris; it now resides in the Louvre. The statue depicts the goddess Nike descending to the prow of a ship to commemorate a victorious naval battle. Inspired by the success and profit of Champoiseau's discovery, the French government sent Gustave Deville and Ernest George Coquart in 1866 to conduct more excavations. Conze returned in 1873 and 1875 and carried out more methodical excavations of the Propylon of Ptolemy II, the Stoa, and partial excavations of the Hieron, the Hall of Choral Dancers, and the Rotunda of Arsinoe. Champoiseau also returned in 1879 and 1891, acquired the base of the Nike statue, and searched for her head. In 1923 and 1927, French-Czechoslovak excavations were led by Antonín Salač, Fernand Chapouthier, and Jan Nepomucký. The Institute of Fine Arts of New York University took over excavations in 1938 under the direction of Karl Lehmann, who was followed by James R. McCredie in 1962. Since the 1950's, the focus has been on excavation, conservation of the site, and in recent years, digital reconstruction.

Today, the Sanctuary of the Great Gods is best known for its magnificent Hellenistic buildings. Most buildings were made of marble which came from a single quarry on Thasos, a neighboring island. Over a dozen buildings of innovative design

were constructed between the mid-4th and late 3rd centuries BCE. Despite the broad sample, there has not yet been an attempt to understand the metric basis for the way in which the buildings were designed. At a site like the Sanctuary of the Great Gods, in which the buildings were constructed within a fairly narrow period and the main material came from the same quarry, we want to determine if the buildings were designed according to an indivisible unit of measure (a *quantum*).

1.2 The Study

The purpose of this study is to use the cosine quantogram method developed by D. G. Kendall (1974) to determine if there are differences in the fundamental quantum underlying the design and construction of two Doric structures in the Sanctuary: the Dedication of Philip III and Alexander IV and the Hieron. Whereas the quantum for length is generally established in Roman and Egyptian metrology due to the survival of measuring rods, it is more difficult to establish Greek metrology (Chippendale, 1986; Wilson Jones, 2000). Weight quanta are also easier to establish in the ancient world due to the discovery of unit weights (Chippendale, 1986). Certain regions do appear to employ specific units of length and there are several established Greek foot-lengths (Rottländer, 1996; Wilson Jones, 2000). However, for regions that do not have established measurement units, the evidence of a length quantum must then be deduced from architectural components.

The Dedication of Philip III and Alexander IV (the *Dedication*) was constructed between 323 and 317 BCE using Pentelic marble on the front façade and Thasian marble on the three remaining walls. This structure was dedicated to the Great Gods by the joint successors of Alexander the Great: Philip III, his half-brother; and Alexander IV, his posthumous son. From the restored plan, the width of the front façade measures 11.01 meters and the length front-to-back is ca. 8.95 meters. These

measurements are at the level of the stylobate – the floor level of the temple. Although the exact function of the Dedication is unknown, it is likely that it was a pavilion for distinguished visitors to observe the proceedings conducted in the Theatral Circle, where the preparations for the initiation rites occurred (Wescoat, forthcoming). The Dedication also included a porch of the Ionic order appended to its west side. Because this addition is later in date and may have a been designed using a different quantum, measurements from this structure were not included in this analysis.

The Hieron, whose name means 'sacred place,' was constructed between 325 and 150 BCE. The addition of a colonnade and completion of the roof account for the large span of construction time (Matsas & Bakirtzis, 2001). Like the Dedication, the dominant building material used was Thasian marble. It measures about 39.25 meters north-to-south by 13 meters east-to-west and was 10.72 meters tall. According to P. W. Lehmann (1969b), it was used for the initiation into the *epopteia*, the highest order of the Mysteries, which included rites of confession and purification. Not including the foundation, about 800 surviving blocks are attributed to this structure.

The Dedication and the Hieron are ideal for analysis because they were constructed using marble, which allows for precise cuts. Marble was quarried off-island; Pentelic marble comes from Mount Pentelicus near Athens and Thasian marble comes from Thasos, near Samothrace. Other structures in the Sanctuary, such as the Stoa, were constructed using porous limestone blocks that were then covered with plaster. This post-treatment of the exterior walls concealed measurement errors made at the quarry or by masons at the site. Measurements from the Doric order are ideal for calculating a quantum because the components used to construct temples were fairly standardized by 600 BCE (Janson & Janson, 2001). Art and architecture of the Ancient Greeks were designed applying the concept of *symmetria*, the foundation of proportional aesthetics based on geometry (Wilson Jones, 2000). By the time of the

Roman Republic, the idea of a quantum existed. Vitruvius, the Roman architect, in Book IV of *De architectura* (ca. 27 BCE), outlines the specific rules of Doric symmetry. Vitruvius mentions the existence of a module – which is similar to a quantum except that it may be subdivided – upon which all temples are designed. Given the evidence for a quantum's existenceand the clear indication from other structures that the Greeks, at least in part, designed their buildings using units of measure, can a quantum be identified for the buildings in the Sanctuary?

Calculating quanta is not a theoretical exercise without practical value. From the estimated quantum, insight into the origin of the architect can be determined. If the proposed quantum is close to or a divisor of an established quantum of a particular region, it may indicate that the architect is from that region. Also, since measurement systems change over time, determination of a quantum could establish a time frame for a building's design and construction. Moreover, identifying a quantum can aid in the process of reconstruction by helping to determine the dimension of missing elements.

1.3 Literature Review

So far, research into statistical analysis of quanta has been limited to merely determining if a quantum exists in a sample and calculating that quantum. Originally, the problem was applied to the topic of atomic weights of chemical elements. In 1815 William Prout hypothesized that since atomic weights of elements measured up to that point are integer multiples of the atomic weight of hydrogen, 1.0079, it must be the element from which all other elements are formed. However, this conclusion was incorrect and was disproved, leading to further conjecture on the quantum for atomic weights. Richard von Mises (1918) applied statistical techniques to the problem by developing the von Mises distribution, which is a circular analog to the normal dis-

tribution for linear data. Francis Aston (1920), inventor of the mass spectrometer, observed that all atomic weights so far measured, except for hydrogen, were multiples of $\frac{1}{16}$ the weight of oxygen (15.9994). This discovery became known as the Whole Number Rule.

The use of statistical methods for calculating archaeological quanta was introduced by A. Thom (1955) in order to determine the Megalithic yard from British stone circles similar to Stonehenge and circles found at Avebury. This method was based on S. R. Broadbent's observation that multimodal data with peaks at evenly-spaced intervals support the existence of a quantum (1955). Broadbent had two methods for determining a quantum based on minimizing the mean squared error (MSE) of the equation $y_{rs} = \beta + rq + \varepsilon_{rs}$, where y_{rs} is the s^{th} stone circle's diameter in the r^{th} subdivision of the data, β is the location of the first mode, q is the quantum, and ε_{rs} is the error. One method verifies or refutes whether a hypothesized value of q, $\hat{q}$, is the true quantum; the other method calculates the quantum when no *a priori* knowledge of q is given (1955; 1956).

D. G. Kendall (1974) used the cosine quantogram method derived from the von Mises distribution to analyze Thom's stone circle data. This method is similar to Broadbent's method, but it assumes a zero intercept ($\beta = 0$). Although Kendall used Monte Carlo simulations to construct a test that a quantum exists, he did not calculate confidence intervals for the point estimate nor did he construct an objective test for comparing quanta from his two regions: England/Wales and Scotland, which he concludes could have different quanta. J. T. Kent (1975) and Csörgő (1980) found that the cosine quantogram equation converges weakly to a simple Gaussian process. Bayesian methods developed by P. R. Freeman (1976) have also been applied to Thom's Megalithic yard problem, which supported Kendall's claim that the quantum based on the Scottish circles was 1.658 meters, but did not support Thom's conclusion

that the stone rows show evidence of a 0.829-meter Megalithic yard. The cosine quantogram method has also been applied to the weight systems of the Ashanti people of Ghana (Hewson, 1980). The methods of Broadbent, Kendall, and Freeman are summarized in M. Baxter's *Statistics in Archaeology* (2003).

Recent research by classicist J. Pakkanen has focused on determining the design unit in Ancient Greek architecture using the cosine quantogram method. He concluded that the quantum underlying the design of the Erechtheion in Athens is 0.3242 meters based on a sample size of 19 measurements on individual blocks (2002). This quantum differs only slightly from the ca. 0.326-meter Doric foot (Dinsmoor, 1961). The Early Iron Age building of the Toumba cemetery at Lefkandi, located on the Greek Island of Euboea, is another focus of Pakkanen's research into design units using the cosine quantogram method. Pakkanen (2004b) concludes that the quantum for this building is between 0.485 and 0.493 meters. For the Temple of Zeus at Stratos, there are three proposed quanta. Courby and Picard (1924) proposed a quantum of 0.316 meters that W. Koenigs (1979) supported, Mertens (1981) proposed the Doric foot, and Bankel (1984) proposed the 0.294-meter Ionic foot. Pakkanen (2004a) finds evidence of another possible quantum using the cosine quantogram method: 0.1053 meters (significant at the $\alpha = 0.05$ level). Pakkenen notes that this value is equal to roughly one third of the 0.316-meter quantum proposed by Courby and Picard. In Pakkanen's study of the Temple of Athena Alea at Tagea, the quantum derived from block dimensions is around 0.099 meters, or roughly one third of the Ionic foot (2005).

Currently, metrological studies have been primarily concerned with determining a quantum and, as a secondary goal, determining if the result is statistically significant based on a distribution of data resembling the sample but not governed by a quantum. However, no studies have delved into the subject of statistically significant differences

between quanta of buildings employing similar design principles at the same site nor have they included any procedure for calculating confidence intervals of point estimates. The objective of this project is to develop a generalized approach to comparisons between buildings and to supplement point estimates with confidence intervals.

2 Methods

2.1 The Sample

Types of blocks included in the dataset were those most likely to have standardized measurements due to their uniformity in their respective buildings. Two types of structural elements were considered: wall blocks and frieze elements. Wall blocks make up the major sides of each building and may be further classified as stretchers, binders, or corner blocks. The latter category may also be further classified as stretcher or binder corner blocks. Exterior walls are constructed using alternating rows of stretcher and binder blocks. Stretchers tend to have heights around 0.5 meters while binders tend to be shorter with heights between 0.225 and 0.275 meters. Architrave wall blocks were also included, because the architrave has similar structural and design standards as the main walls. Binders from the string course and the epikranitis of the Dedication were also included. However, wall blocks from the orthostate were excluded. Apse wall blocks from the Hieron were also excluded because different design principles govern the construction of the apse. Wall blocks were chosen for analysis because of their consistent dimensions and their abundance in the dataset to avoid issues with small sample sizes.

The other type of blocks most likely to be cut using a quantum are frieze elements: triglyphs, metopes, mutules, and regulae. Triglyphs are made up of three channels (*glyphs*) and three ridges (*femora*) arranged as half-glyph, femur, glyph, femur, half-glyph. In between two triglyphs is a metope, which could be plain, painted, or have embellishments in relief. In this period in Greek architecture, each triglyph should have approximately the same dimensions as every triglyph in the structure; each metope should have approximately the same dimensions as every metope. The combination of a triglyph with its adjacent metope is known as a frieze unit. The frieze

contains a periodic pattern of the frieze unit motif repeated symmetrically around the perimeter of the building. It is from this strict symmetry that the mathematical concepts of frieze patterns and frieze groups are derived. Assuming plain metopes, the frieze unit motif belongs to the frieze group applying horizontal translation (i.e., the frieze unit is repetitively shifted horizontally in one direction). Mutules are part of the underside of horizontal geison blocks and are located above and in line with the triglyphs and the center line of the metopes. Regulae are ornamental portions of the architrave and are located below the triglyphs and metopes. The lengths of these elements are the same as the lengths of their corresponding triglyphs and therefore add similar dimensions to the dataset. Sources of information on mutule and regula lengths include: architrave wall blocks, epistyle blocks, and horizontal and lateral geison blocks. Triglyph and metope heights and lengths were included, when available, as well as lengths of mutules and regulae.

Block measurements used in this study came from two sources: blocks from the Dedication were measured by a team led by Bonna Wescoat of Emory University; blocks from the Hieron came from Volume III (Plates) of the Samothrace publication series (P. W. Lehmann, 1969a). In order to measure the coarse block surfaces, metal angles made of either steel or aluminum were used to simulate a smooth surface by touching down on several points of the original surface. When measuring whole blocks, the thin side of two metal angles (*steels*) were positioned at the same place on each end of the desired dimension. The distance between the two steels was then measured using a metal metric measuring tape. Blocks were selected for inclusion in the Hieron volume by Lehmann if they represented ideal or unbroken blocks of the structure. Additionally, Wescoat's team has remeasured blocks of the Hieron, but these measurements are not currently in the dataset because they must be checked against Lehmann's Hieron volume first. Blocks must have at least one complete dimension

to be included in the final dataset. Analysis did not include broken dimensions (i.e., censored observations) because they do not contribute to a reliable estimate of the quantum.

2.2 Block Dimensions

Blocks are measured across three dimensions: height, length, and width. Height is defined as the vertical dimension on the block that extends from the floor of the building to the roof. The length of a block is the horizontal breadth on the outer façade to the floor. The block's width is how deep the block extends from the exterior into the interior of the building. Because the wall depth in Doric buildings is not consistent throughout the building, widths were excluded from analysis. The data have been collapsed across dimension so that each measurement is not distinguishable between height and length. However, the model given below can be easily generalized to include information on dimension.

2.3 Quantum Model

A quantum is formally defined as the smallest unit common to a set of measurements of size n such that each measurement is a positive integer multiple of the quantum itself, represented by

$$y_i = qM_i + \varepsilon_i, \quad i = 1, 2, \ldots, n \tag{1}$$

where y_i is the observed length of block i with a fixed dimension, q is the quantum, M_i is a positive integer,[1] and ε_i is the error.[2] This model is the foundation for deriving the cosine quantogram equation. Suppose the measurement data are marked on a piece

[1] $M_i \in \mathbb{Z}^+ = \{1, 2, 3, \ldots\}$

[2] The error term may then be calculated for each measurement i by exploiting the nature of M_i. Because $M_i \in \mathbb{Z}^+$, ε_i is the solution of $y_i \bmod q$

of tape starting at one end. Suppose there is also a circle of circumference equal to C. When the tape is wrapped around the perimeter of the circle, and if a quantum exists for the data and is equal to C, the markings should cluster around the zero-point of the circle. The distribution formed is known as the von Mises distribution (Kendall, 1974). The von Mises distribution is similar to the wrapped normal distribution, which is a version of the normal distribution around a unit circle ($C = 2\pi$). Thus, the error term is assumed to be distributed von Mises.

2.4 Calculations

2.4.1 Cosine Quantogram

Kendall (1974) defined the cosine quantogram equation used to find the quantum q as:

$$\phi\left(\frac{1}{q}\right) = \sqrt{\frac{2}{n}} \sum_{i=1}^{n} \cos\left(\frac{2\pi y_i}{q}\right) \tag{2}$$

The quantum of the data, if it exists, is found by calculating $\phi\left(\frac{1}{q}\right)$ over a range of values of q and determining the value of q that maximizes $\phi(\cdot)$, $\hat{q}$. Kendall uses the term $\sqrt{\frac{2}{n}}$ to add a dependence on the sample size and to allow the cosine quantogram to approach a standard normal distribution for moderate values of n and q. However, since this factor does not depend on q and we are only concerned with the value of $\hat{q}$, not $\phi\left(\frac{1}{\hat{q}}\right)$ itself, it may be eliminated from calculations of the cosine quantogram. The other portion of the quantogram, $\cos\left(\frac{2\pi y_i}{q}\right)$, may also be written in terms of the error as $\cos\left(\frac{2\pi \varepsilon_i}{q}\right)$, because y_i is equal to $qM_i + \varepsilon_i$ and $M_i \in \mathbb{Z}^+$ from equation (1). This quantity is proportional to the von Mises probability density, which is essential for constructing a test statistic for hypothesis testing.

2.4.2 Lower and Upper Bounds of q

In order to exclude nonsensical quanta, lower and upper bounds were placed on possible values of q. The metrological relief from Salamis and the Oxford metrological relief, most likely found in western Asia Minor or a nearby island, demonstrate that measurement systems based on body proportions were common (Wilson Jones, 2000). Because cubits based on six human palm lengths, or 24 fingers (*dactyls*),[3] were pervasive units throughout Ancient Greece and Rome, these lower and upper limits on possible values of q are based on previously defined dactyls and cubits. The procedure for finding an appropriate lower bound captures the estimate of the dactyl, while the procedure for finding the upper bound captures the estimate of the cubit, based on a flowchart from Rottländer (1996) and Wilson Jones (2000) (Tables 1 and 2). The lower bound is 90% smaller than the smallest dactyl. Dactyls are found reliably from foot measurements: there are 16 dactyls in a foot. The smallest dactyl, 0.0144 meters, is derived from the Earth foot (Table 2). The upper bound is 110% larger than the largest cubit in Table 1, one of two Late Egyptian cubits (0.5417 meters). The lower and upper bounds of q are, therefore, 0.013 meters and 0.596 meters. The cosine quantogram was calculated with millimeter precision.

2.4.3 Unrounding

In order to account for measurement error committed by archaeologists, measurements were 'unrounded' before analysis according to Kendall's recommended method (1974). Measurements ranged in precision from the nearest tenth of a meter (decimeter) to the nearest thousandth of a meter (millimeter). The process of unrounding involves adding a random value within $[-0.05, 0.05)$ for measurements rounded to the nearest decimeter, a random value within $[-0.005, 0.005)$ for measurements rounded

[3]Equivalently, a cubit is the length of the forearm from the elbow to the tip of the middle finger

Table 1: Table of Cubits (Ordered from Largest to Smallest)

Type	**Length (meters)**
Late Egyptian cubit (A)	0.5417
Late Egyptian cubit (B)	0.5363
Great Ptolemaic cubit	0.5332
Great Egyptian Royal cubit	0.5289
'New cubit'	0.5270
Egyptian Royal Cubit	0.5236
'Compromis' cubit	0.5210
Nippur cubit	0.5184
Salamis cubit	0.4838
Cubitus Romanus	0.4444

Table 2: Table of Dactyls (Ordered from Largest to Smallest)

Type	**Length (meters)**	**Dactyl Length (meters)**
Great Ptolemaic foot	0.3554	0.0222
Samian-Ionian foot	0.3477	0.0217
Indus foot	0.3456	0.0216
Cretan-Aeginetan foot	0.3332	0.0208
Drusian foot	0.3332	0.0208
Doric-Pheidonic foot	0.3269	0.0204
Pied du roi	0.3248	0.0203
Byzantine foot	0.3206	0.0200
Milesian foot	0.3173	0.0198
Common Greek foot	0.3160	0.0198
'Eginean' foot	0.3142	0.0196
Attic-Olympic foot	0.3110	0.0194
Small Ptolemaic foot	0.3086	0.0193
pes Romanus	0.2962	0.0185
Attic-Cycladic foot	0.2943	0.0184
Punic foot	0.2941	0.0184
Vindonissa foot	0.2925	0.0183
Oscian-Umbrian foot	0.2757	0.0172
Gudea foot (ideal)	0.2654	0.0166
Gudea foot (real)	0.2646	0.0165
Pythic foot	0.2488	0.0156
Earth foot	0.2304	0.0144

to the nearest centimeter, and so on. Therefore, if the newly unrounded measurement is rounded to the same decimal place as the original value, it would be rounded up or down to the original value. A formula for unrounding the data is:

$$y_{i,unrounded} = y_i + \left(0.5 \times 10^{-\nu_i}\right) \cdot U,$$

where ν_i is the number of decimal places of measurement i and U is a random number from a $UNIF(0, 1)$ distribution.

During the measuring phase, some block dimensions appeared to be between two measurements at the millimeter level, so the arithmetic mean of the two measurements was recorded. These measurements were treated as though they were accurate to the last decimal place given. Approximations at that level are unlikely to affect the quantal estimates since unrounding using a random fraction of ± 0.0001 should adequately account for any error.

2.5 Hypothesis Testing

The next step from Kendall's method is to construct significance tests between subgroups of the dataset. The simple model (1) can be generalized to provide for a better description of the data:

$$y_{ijk} = q_{ij} M_{ijk} + \varepsilon_{ijk}, \tag{3}$$

where i is redefined from earlier as the building index ($i = 1$ is the Dedication, $i = 2$ is the Hieron), j is the block type index ($j = 1$ is wall blocks, $j = 2$ is frieze elements), and k indexes each measurement in a set of n measurements ($k \in \{n_{\cdot\cdot}, n_{i\cdot}, n_{\cdot j}, n_{ij}\}$). From this equation, the cosine quantogram (2) can also be generalized to include

information on buildings and block types:

$$\phi\left(\frac{1}{q_{ij}}\right) = \sqrt{\frac{2}{n}} \sum_{k=1}^{n} \cos\left(\frac{2\pi y_{ijk}}{q_{ij}}\right), \tag{4}$$

for every i, j, and k. The hypotheses of interest are whether the quanta calculated for each building, the Dedication and the Hieron, are equal and whether the quanta calculated for each block type are equal given that they come from the same building. Only two-sided tests were of interest because there was no reason to suspect that one quantum should be larger than the other *a priori*.

Assuming a von Mises distribution, we may construct likelihood functions of the data under H_0 and H_A for each test, take the ratio and compare it to a pre-specified critical value based on the bootstrap distribution of $\hat{q}^*$. For the von Mises distribution with mean direction μ and concentration parameter κ, the probability density function of $VM(\mu, \kappa)$ for angle θ is

$$f\left(\theta; \mu, \kappa\right) = \frac{1}{2\pi I_0(\kappa)} e^{\kappa \cos(\theta - \mu)}, \tag{5}$$

where $I_0(\cdot)$ is the modified Bessel function of the first kind and order zero. The parameters μ and κ are similar to the mean and variance of a normal distribution, respectively. The mode of the distribution occurs at μ, which represents the mean direction from the zero-point on the circle that values of angle θ take. Parameter κ is analogous to $1/\sigma^2$; larger values of κ indicate distributions with higher peaks and less spread while smaller values of κ indicate distributions with lower peaks and more spread at a given value of μ. If $\kappa = 0$, the distribution is uniform on the circle.

The objective of the first hypothesis test is to determine if the quantum from each building's marginal distribution is equal to the quantum for the joint distribution; that is, if the quantum for each building is equal to the quantum calculated for

both buildings. The simple null hypothesis and composite alternative hypothesis are, therefore,

$$H_0 : q_{\cdot\cdot} = q_{i\cdot},$$

for all buildings i

$$H_A : q_{\cdot\cdot} \neq q_{i\cdot},$$

for at least one building i. Denote the likelihood under the null hypothesis as $L\left(Y|H_0\right)$ and the likelihood under the alternative hypothesis as $L\left(Y|H_A\right)$. Because the cosine quantogram equation is proportional to the von Mises distribution, the likelihood ratio is

$$LR_1 = \frac{L\left(Y|H_0\right)}{L\left(Y|H_A\right)} = \frac{\sup_{q_{ij}|q_{\cdot\cdot}=q_{i\cdot},\forall i} \prod_i \prod_j \prod_k \exp\left(\kappa \cos\left(\frac{2\pi\varepsilon_{ijk}}{q_{ij}}\right)\right)}{\sup_{q_{ij}} \prod_i \prod_j \prod_k \exp\left(\kappa \cos\left(\frac{2\pi\varepsilon_{ijk}}{q_{ij}}\right)\right)},$$

for building i, block type j, and measurement k. The test statistic is the logarithm of the likelihood ratio, given by

$$LLR_1 = \sum_i \sum_j \sum_k \exp\left(\kappa \cos\left(\frac{2\pi\hat{\varepsilon}^*_{ijk}}{\hat{q}^*_{\cdot\cdot}}\right)\right) - \sum_i \sum_j \sum_k \exp\left(\kappa \cos\left(\frac{2\pi\hat{\varepsilon}^*_{ijk}}{\hat{q}^*_{i\cdot}}\right)\right)$$

for building i, block type j, and measurement k. The parameter $\hat{q}^*$ is estimated from the resampled data and $\hat{\varepsilon}^*$ is the error calculated from the resampled data. If the log-likelihood ratio is greater than a specified critical value, then the null hypothesis may be rejected in favor of the alternative hypothesis.

The second hypothesis test of interest determines if the quanta calculated for the marginal distributions of wall blocks and frieze elements equals the joint distribution of blocks in the Dedication only; that is, if the quanta for the wall blocks and for the frieze elements in the Dedication are equal to the quantum associated with all blocks

in the Dedication. The null and alternative hypotheses are:

$$H_0 : q_{1\cdot} = q_{1j},$$

for block types j in the Dedication and

$$H_A : q_{1\cdot} \neq q_{1j},$$

for at least one block type j in the Dedication. The log-likelihood ratio is, therefore,

$$LLR_2 = \sum_i \sum_j \sum_k \exp\left(\kappa \cos\left(\frac{2\pi\hat{\varepsilon}^*_{1jk}}{\hat{q}^*_{1\cdot}}\right)\right) - \sum_i \sum_j \sum_k \exp\left(\kappa \cos\left(\frac{2\pi\hat{\varepsilon}^*_{1jk}}{\hat{q}^*_{1j}}\right)\right),$$

for block type j, and measurement k of the Dedication.

Similarly, the third hypothesis test determines if the quanta for the wall blocks and for the frieze elements in the Hieron are equal to the quantum associated with all blocks in the Hieron. The null and alternative hypotheses are:

$$H_0 : q_{2\cdot} = q_{2j},$$

for block types j in the Hieron and

$$H_A : q_{2\cdot} \neq q_{2j},$$

for at least one block type j in the Hieron. The test statistic is, therefore,

$$LLR_3 = \sum_i \sum_j \sum_k \exp\left(\kappa \cos\left(\frac{2\pi\hat{\varepsilon}^*_{2jk}}{\hat{q}^*_{2\cdot}}\right)\right) - \sum_i \sum_j \sum_k \exp\left(\kappa \cos\left(\frac{2\pi\hat{\varepsilon}^*_{2jk}}{\hat{q}^*_{2j}}\right)\right),$$

for block type j and measurement k of the Hieron.

In all tests, the value of κ is unknown. Because κ is a nuisance parameter, the log-likelihood ratio cannot be compared to a critical value from a pre-specified distribution. However, κ may be factored out without loss of power, and the quantity $C_t = \frac{1}{\kappa} LLR_t$ for tests $t = 1, 2, 3$ can become the test statistic:

$$C_1 = \frac{LLR_1}{\kappa} = \sum_i \sum_j \sum_k \exp\left(\cos\left(\frac{2\pi\hat{\varepsilon}^*_{ijk}}{\hat{q}^*_{\cdot\cdot}}\right)\right) - \sum_i \sum_j \sum_k \exp\left(\cos\left(\frac{2\pi\hat{\varepsilon}^*_{ijk}}{\hat{q}^*_{i\cdot}}\right)\right)$$

$$C_2 = \frac{LLR_2}{\kappa} = \sum_i \sum_j \sum_k \exp\left(\cos\left(\frac{2\pi\hat{\varepsilon}^*_{1jk}}{\hat{q}^*_{1\cdot}}\right)\right) - \sum_i \sum_j \sum_k \exp\left(\cos\left(\frac{2\pi\hat{\varepsilon}^*_{1jk}}{\hat{q}^*_{1j}}\right)\right)$$

$$C_3 = \frac{LLR_3}{\kappa} = \sum_i \sum_j \sum_k \exp\left(\cos\left(\frac{2\pi\hat{\varepsilon}^*_{2jk}}{\hat{q}^*_{2\cdot}}\right)\right) - \sum_i \sum_j \sum_k \exp\left(\cos\left(\frac{2\pi\hat{\varepsilon}^*_{2jk}}{\hat{q}^*_{2j}}\right)\right)$$

Critical values for the log-likelihood ratios may be found by resampling, generating LLRs for each replicate sample, and creating a set of sufficiently numerous percentiles to arrive at a well-defined distribution for the LLRs ($PCTL = 0.5x$, $x = (0, 1, 2, \ldots, 200)$). The p-value for the test is the probability under the null hypothesis of obtaining an LLR at least as extreme as the original, so $p = 100 - PCTL$. The distribution of percentiles (p-values) is discrete, so linear interpolation should be used to calculate the p-value. This equation is given by

$$p_t = p_L + (C_t - C_L)\,\frac{p_U - p_L}{C_U - C_L},$$

where C_t is the test statistic of test t and p_t is its corresponding p-value. (C_L, p_L), and (C_U, p_U) are the lower and upper neighboring critical values of (C_t, p_t), respectively.

2.5.1 Monte Carlo Simulations and Bootstrapping

Monte Carlo methods were used to calculate confidence intervals and to conduct hypothesis tests. In general, Monte Carlo methods compare the original sample to a

distribution from an assumed model. A bootstrap test is a special case of the Monte Carlo test. The basis of bootstrapping is random sampling from the original dataset. If the original sample is of size n, then N resamples also of size n are taken using unrestricted random sampling (i.e., sampling with replacement). Unrestricted random sampling gives each observation an equal probability of selection. This resampling method is particularly helpful if the parameter of interest is from an unknown distribution. The more random samples are generated, the faster the bootstrap distribution converges to the actual distribution of the parameter.

In order to construct an accurate distribution for the data, $N = 10,000$ samples were taken, stratified by both building and block type to ensure that the proportions of measurements from the same building and type are equal to those from the original dataset for each subset of the data. The unrounding procedure was performed on each replicate sample. From the replicate samples, the standard deviation of the collection of point estimates $\hat{q}^*$ from each sample approximates the standard error of the underlying distribution. Marriott (1979) provides a formula for determining the number of simulations, N, needed to reject H_0 of one-sided tests. However, we are concerned with two-sided hypothesis tests. We only consider large values of N (such that $Npq > 5$), so the normal approximation to the binomial distribution of the probability of rejecting H_0 may be used:

$$P \approx P_L + P_U,$$

where

$$P_L \approx 1 - \Phi\left(\frac{(N+1) - m_L - \frac{1}{2} - Nq}{\sqrt{Npq}}\right)$$

and

$$P_U \approx 1 - \Phi\left(\frac{(N+1) - m_U - \frac{1}{2} - Nq}{\sqrt{Npq}}\right)$$

where N is the number of simulations, $p = \frac{\alpha}{2}$, $q = 1 - \frac{\alpha}{2}$, $m_L = \frac{\alpha}{2}(N+1)$ and $m_L = \left(1 - \frac{\alpha}{2}\right)(N+1)$, and $\Phi(\cdot)$ is the cumulative distribution function of a normal distribution. The continuity correction of $\frac{1}{2}$ is needed to convert from a discrete distribution to a continuous one. Table 3 summarizes the probability of rejecting H_0

Table 3: Probability of Rejecting H_0 in Monte Carlo Tests

	p								
N	**0.070**	**0.065**	**0.060**	**0.055**	**0.050**	**0.045**	**0.040**	**0.035**	**0.030**
500	0.091	0.143	0.219	0.319	0.446	0.592	0.741	0.868	0.952
1000	0.036	0.077	0.155	0.283	0.462	0.667	0.847	0.955	0.993
2500	0.003	0.015	0.064	0.205	0.476	0.782	0.957	0.997	1.000
5000	0.000	0.001	0.017	0.131	0.483	0.874	0.993	1.000	1.000
10,000	0.000	0.000	0.002	0.060	0.488	0.951	1.000	1.000	1.000

given that the actual p-value is 0.05. From this table, it appears that $N = 1000$ simulations is adequate because the probability of rejecting H_0 is greater than 80% when p is very close to 0.05 (such as when $p = 0.045$); however, larger numbers of simulations give even better results and do not drastically increase computing time. For example, the probability of rejecting H_0 when $p = 0.045$ is 0.95 – very close to one.

Confidence intervals will be calculated using the standard bootstrap method. The quantum, or any statistic, is calculated for each of the N replicate samples and the standard error is found from this distribution. The assumptions of the standard bootstrap confidence interval are:

1. $\hat{q}$ is approximately normally distributed
2. $\hat{q}$ is unbiased
3. Bootstrap resampling provides a good approximation for the standard deviation of q, σ (Manly, 2007).

If these assumptions hold, then a $100(1-\alpha)\%$ confidence interval for q takes the form $\hat{q} \pm z_{\alpha/2}\hat{\sigma}$, where $\hat{\sigma}$ is estimated from the collection of bootstrap estimates of q. Therefore, a 95% confidence interval for q is $\hat{q} \pm 1.96\hat{\sigma}$.

2.6 Diagnostics

2.6.1 Conversion of Linear Data to Circular/Angular Data

In order to perform other tests on the data, such as goodness-of-fit tests and significance tests on parameters of the von Mises distribution of the errors, the linear data must first be converted into circular data. For each subset of the data (i.e., data from either building, and data from either types of blocks from each building), the calculated quantum will be assumed to be the true quantum of the data. From these quanta, circles with circumferences equal to $\hat{q}$ may be constructed upon which the inferred von Mises distribution lies. Returning to the indexing conventions in equations (1) and (2), for each unrounded measurement y_i, the calculated error is equivalent to arc length. In general, an angle $\angle\theta_i$, in radians, is derived from the linear measurement from the formula $\angle\theta_i = \frac{2\pi y_i}{\hat{q}}$, where $i = 1, 2, \ldots, n$.

2.6.2 Goodness-of-Fit Tests

To confirm that the calculated quanta are valid, the assumption that the data are from a von Mises distribution will be tested using a goodness-of-fit test that was derived by Watson (1961) and expanded by Lockhart and Stephens (1985). Because both μ and κ are unknown parameters, they must be estimated using their maximum likelihood estimates (MLEs). The MLE for μ ($\hat{\mu}$) is the direction of the resultant (R) of the vectors formed from the origin O to a point on the circle P_i for every observation i. The MLE of κ is $\hat{\kappa} = A^{-1}(\bar{R})$ (i.e., the inverse of the ratio of the first and

zeroth order Bessel functions evaluated at the value of $\bar{R}$, the mean resultant length). After estimating these parameters, $z_i = F(\theta_i; \mu, \kappa)$, where $F(\cdot)$ is the cumulative density function of the von Mises distribution, is calculated. Next, the order statistics $\left(z_{(1)}, z_{(2)}, \ldots, z_{(n)}\right)$ are obtained for z_i. The statistic U^2 is then calculated where

$$U^2 = \sum_{i=1}^{n} \left\{ \left(\frac{z_{(i)} - (2i-1)}{2n} \right)^2 \right\} - n\left(\bar{z} - \frac{1}{2}\right)^2 + \frac{1}{12n}$$

and is compared to critical values. Because results of goodness-of-fit tests in smaller samples are more sensitive to slight departures from the distribution, only the marginal distributions of the buildings will be tested.

2.6.3 Significance Testing for μ (κ Unknown)

If the estimates $\hat{q}$ are appropriate, the mean of the errors for each subset should be equal to zero. Therefore, the null hypothesis is that $\mu = 0$ and the alternative hypothesis is that $\mu \neq 0$. Let $C = \sum_{i=1}^{n} \cos\theta_i$ and $\bar{C} = \frac{C}{n}$. Because κ is unknown and n is not large for all subsets, but $n > 5$, an approximate likelihood ratio statistic is:

$$W = \begin{cases} \frac{2n^3}{n^2 + C^2 + 3n} \log \frac{1-\bar{C}^2}{1-\bar{R}^2} & \text{if } \bar{C} > \frac{2}{3} \\ \frac{4n\left(\bar{R}^2 - \bar{C}^2\right)}{2-\bar{C}^2} & \text{if } \bar{C} \leq \frac{2}{3} \end{cases},$$

(Mardia & Jupp, 2000; Upton, 1973). This statistic is asymptotically distributed χ_1^2.

2.6.4 Homogeneity between Pairs of Subsets

The homogeneity between pairs of distributions will be tested using Watson's two-sample test, which checks whether the data from two samples come from the same population (Jammalamadaka, 2001). In general, the test takes the form $H_0 : F_1 = F_2$ where F_1 and F_2 are the empirical density functions of distributions of size n_1 and

n_2, respectively, such that $n = n_1 + n_2$. This test assumes that $\kappa_1 = \kappa_2$ (Mardia & Jupp, 2000). We will test to see if the data from the Dedication and the Hieron come from the same population and also if the measurements from different block types within a building come from the same population. The three tests are $H_0 : F_{1\cdot} = F_{2\cdot}$, $F_{11} = F_{12}$, and $F_{21} = F_{22}$ versus their corresponding two-tailed alternatives.

2.7 Software Packages

Univariate analysis and cosine quantogram analysis were performed using SAS version 9.2. Analysis of circular data was done using R version 2.6.2 and using the circular package version 0.3-9 developed by Claudio Agostinelli and Ulric Lund (2007). Plots were generated in R version 2.6.2.

3 Results

Seventy-six blocks were included in the final analysis. Twenty were wall blocks from the Dedication, 24 were frieze elements from the Dedication, 20 were wall blocks from the Hieron, and 12 were frieze elements from the Hieron. In the Dedication, 31 measurements came from wall blocks and 26 measurements came from frieze elements. For the wall blocks there were 20 height measurements and 11 lengths. For the frieze elements, there were 3 heights and 23 lengths, because only the lengths of mutules and regulae were included. In the Hieron, there were 39 measurements from wall blocks: 20 heights and 19 lengths. For the frieze elements, there were 17 measurements: 6 heights and 11 lengths. These data are summarized in Tables 4 and 5.

Table 4: Summary of Blocks Used

Building	**# of Blocks**	**Block Type**	**# of Blocks**
Dedication	44	Wall Blocks	20
		Frieze Elements	24
Hieron	32	Wall Blocks	20
		Frieze Elements	12

3.1 Missing Data

The definition of missing data differs for blocks and measured dimensions. Missing blocks can be blocks that are present in a building's restored plan, but are not present in the dataset. A missing block may also be a block that is present in the dataset, but does not have at least one complete (i.e., unbroken) dimension. Dimensions are considered missing if no value is present or if it is incomplete (i.e., broken). Some blocks contained partial lengths of mutules and regulae that are to be matched with others to form the length of a complete mutule or regula. These dimensions were not

Table 5: Summary of Block Measurements Used

Building	**# of Measurements**	**Block Type**	**# of Measurements**	**Dimension**	**# of Measurements**
Dedication	57	Wall Blocks	31	Height	20
				Length	11
		Frieze Elements	26	Height	3
				Length	23
Hieron	56	Wall Blocks	39	Height	20
				Length	19
		Frieze Elements	17	Height	6
				Length	11

included and were not considered to be broken.

From the reconstructed plan of the Dedication, there are ca. 462 wall blocks and 192 frieze elements. In the dataset, however, there are only 27 wall blocks and 26 frieze elements with at least one dimension value given, either broken or unbroken. Of the 27 wall blocks present, 20 had at least one complete dimension. Of the 33 frieze elements present, 24 had complete dimensions. The percentage of wall blocks used was 4.3% (95.7% missing) and the percentage of frieze elements used was 12.5% (87.5% missing). This difference between proportions was statistically significant at the $\alpha = 0.05$ level ($p = 0.001$). Of the 924 potential measurements from wall blocks (462 heights and 462 lengths), 31 were present. Of the 268 potential frieze element measurements (40 triglyph lengths, 40 triglyph heights, 36 metope lengths, 36 metope lengths, 76 mutule lengths, and 40 regula lengths), 26 were present. The percentage of wall blocks measurements used (3.4% present, 96.6% missing) compared to frieze elements (9.7% present, 90.3% missing) was statistically significant ($p = 0.001$). Wall blocks and measurements from wall blocks tended to be missing more often than frieze elements. From a statistical standpoint, this high percentage of missing data is troubling; however, the percentage of measurements included in the dataset is high for an archaeological study.

There are ca. 688 wall blocks and 432 frieze elements present in the Hieron's reconstructed plan. Twenty wall blocks were present in the dataset and all had at least one complete dimension. There were 13 frieze elements in the dataset, and 12 had at least one complete dimension. In the Hieron, the percentage of wall blocks present was 2.9% (97.1% missing) and the percentage of frieze elements present was 2.8% (97.2% missing). This difference was not statistically significant ($p = 0.899$). Of the 1376 possible wall block measurements (688 heights, 688 lengths), 39 were usable (2.8% non-missing, 97.2% missing). For frieze elements, there are 604 possible

measurements: 88 triglyph lengths, 88 triglyph heights, 84 metope lengths, 84 metope heights, 172 mutule lengths, and 88 regula lengths. Seventeen measurements were usable (2.8% non-missing, 97.2% missing). The diffence between proportions of non-missing measurements between wall blocks and frieze elements was not statistically significant ($p = 0.981$). Similarly, the proportions of usable blocks and measurements may appear to be small to the statistician, but to the archaeologist, these proportions are large.

Differences between proportions of missing/non-missing blocks and measurements in the Dedication and the Hieron is due to the way the data were collected. Blocks of the Hieron were chosen because they represented prototypical blocks; they are far less likely to have any broken dimensions. However, only a few examples of prototypical blocks were given, so similar blocks were not included. Therefore, there tended to be smaller proportions of blocks and measurements from the Hieron compared to the Dedication. A comparison between total blocks used from the Dedication (6.7% present, 93.3% missing)and the Hieron (2.9% present, 97.1% missing) was highly significant ($p < 0.001$). The proportion of usable measurements from the Dedication was 4.8% while the proportion of usable measurements from the Hieron was 2.8%. This difference was statistically significant ($p = 0.007$). These proportions translate to 95.2% and 97.2% missing, respectively.

3.2 Univariate Analysis of Block Subgroups between Buildings

A comparison between the average block dimensions of subgroups of blocks (binders, stretchers, triglyphs, etc.) shows that the properties of blocks used in the Dedication and the Hieron are different. Because the assumption of normality was violated

for most subgroups of blocks, non-parametric tests between buildings were used for consistency and simplicity. Power is reduced when using non-parametric tests on normal data, but there was a statistically significant difference between each subgroup considered at the $\alpha = 0.05$ level (Table 6). The median length of wall blocks from the Dedication was 1.0420 meters and the median length of wall blocks from the Hieron was 1.3100 meters ($p = 0.0017$). Binders tended to have heights between 0.228 and 0.259 meters (interquartile range) in the Dedication and between 0.246 and 0.275 meters in the Hieron (IQR). The median height for binders in the Dedication was 0.2320 meters and 0.2635 for the Hieron ($p = 0.0064$). The heights of stretchers tended to be between 0.474 and 0.478 meters in the Dedication and between 0.564 and 0.586 meters in the Hieron (IQR). The median stretcher height was 0.4750 meters in the Dedication and 0.5720 meters in the Hieron ($p < 0.0001$). The height of triglyphs and metopes in the Dedication was 0.6700 meters and 0.7475 meters in the Hieron ($p = 0.0269$). The triglyph lengths, which include mutule and regula lengths, have medians of 0.4150 meters in the Dedication and 0.4873 meters in the Hieron ($p = 0.0003$).

Table 6: Summary of Measurements of Subgroups of Blocks between Buildings

Block Type (Dimension)		**Dedication**		**Hieron**		p**-value**
		N	**Median**	**N**	**Median**	
Wall Blocks	All (L)	11	1.0420	19	1.3100	0.0017
	Binders (H)	7	0.2320	8	0.2635	0.0064
	Stretchers (H)	11	0.4750	11	0.5720	0.0001
Frieze Elements	All (H)	3	0.6700	6	0.7475	0.0269
	Triglyphs (L)	19	0.4150	4	0.4873	0.0003

3.3 Comparison of Quanta between Buildings

The distribution of all measurements from both the Dedication and the Hieron (Figure 1) suggests that quanta may exist for the two buildings, but that they may not be equal because the modes do not occur at regularly-spaced intervals. The distance between the first and second peaks is 0.622 meters while the distance between the second and third peaks is 0.893 meters. Figures 2 and 3 show the distributions of the data for the Dedication and Hieron, respectively, and also suggest that a quantum may exist for their respective measurements.

The estimate of the quantum q for the Dedication is $\hat{q}_{1\cdot} = 0.211$ meters ($SE = 0.0719$ meters). A 95% confidence interval for $q_{1\cdot}$ is (0.070 m., 0.352 m.). Figure 4 is the plot of the cosine quantogram for the Dedication with a maximum value of $\phi(\cdot)$ occurring at $q = 0.211$ meters. The estimate of $q_{2\cdot}$ for the Hieron is $\hat{q}_{2\cdot} = 0.253$ meters ($SE = 0.0458$ meters). A 95% confidence interval for $q_{2\cdot}$ is (0.163 m., 0.343 m.). Figure 5 is the plot of the cosine quantogram for the Hieron, showing that the ideal quantum is $\hat{q}_{2\cdot} = 0.253$. These results are shown in Table 7. For the test that the quanta for the two buildings are equal, the test statistic T_1 is -13.7929. There is not a statistically significant difference between the at least one of the two quanta and the joint distribution ($p = 0.270$).

Table 7: Comparison of Quanta between Buildings

Building	$\hat{q}$	$SE(\hat{q})$	**95% Confidence Interval**
Dedication	0.211	0.0719	(0.070, 0.352)
Hieron	0.253	0.0458	(0.163, 0.343)

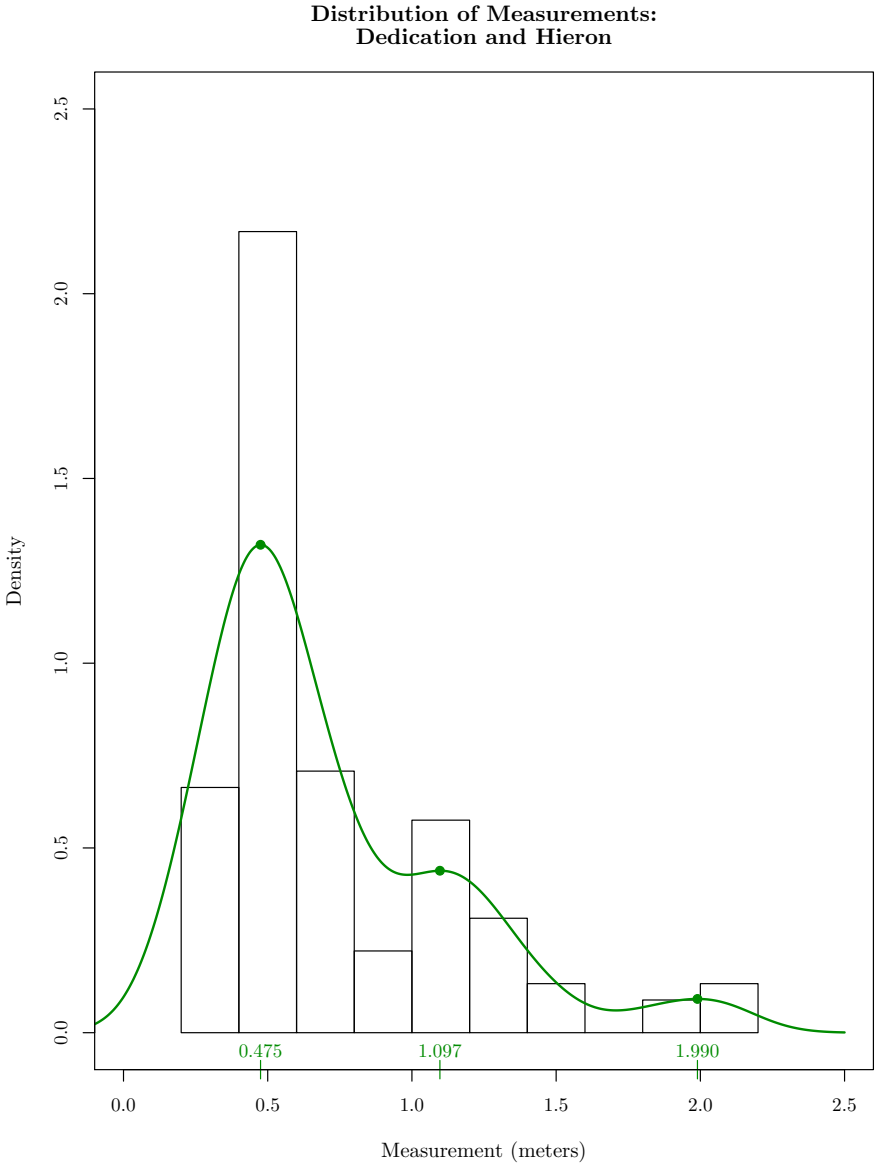

Figure 1: Histogram and KDE Function of Measurements from the Dedication and Hieron

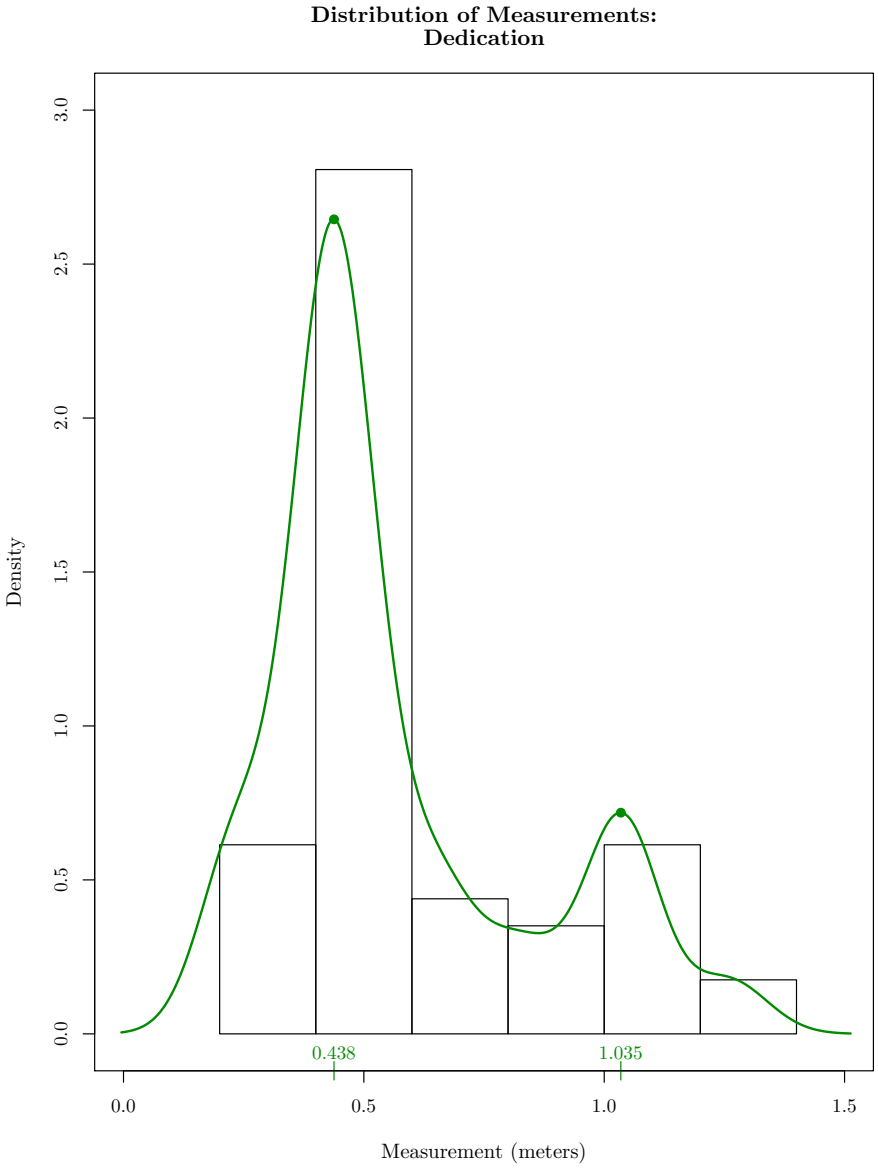

Figure 2: Histogram and KDE Function of Measurements from the Dedication

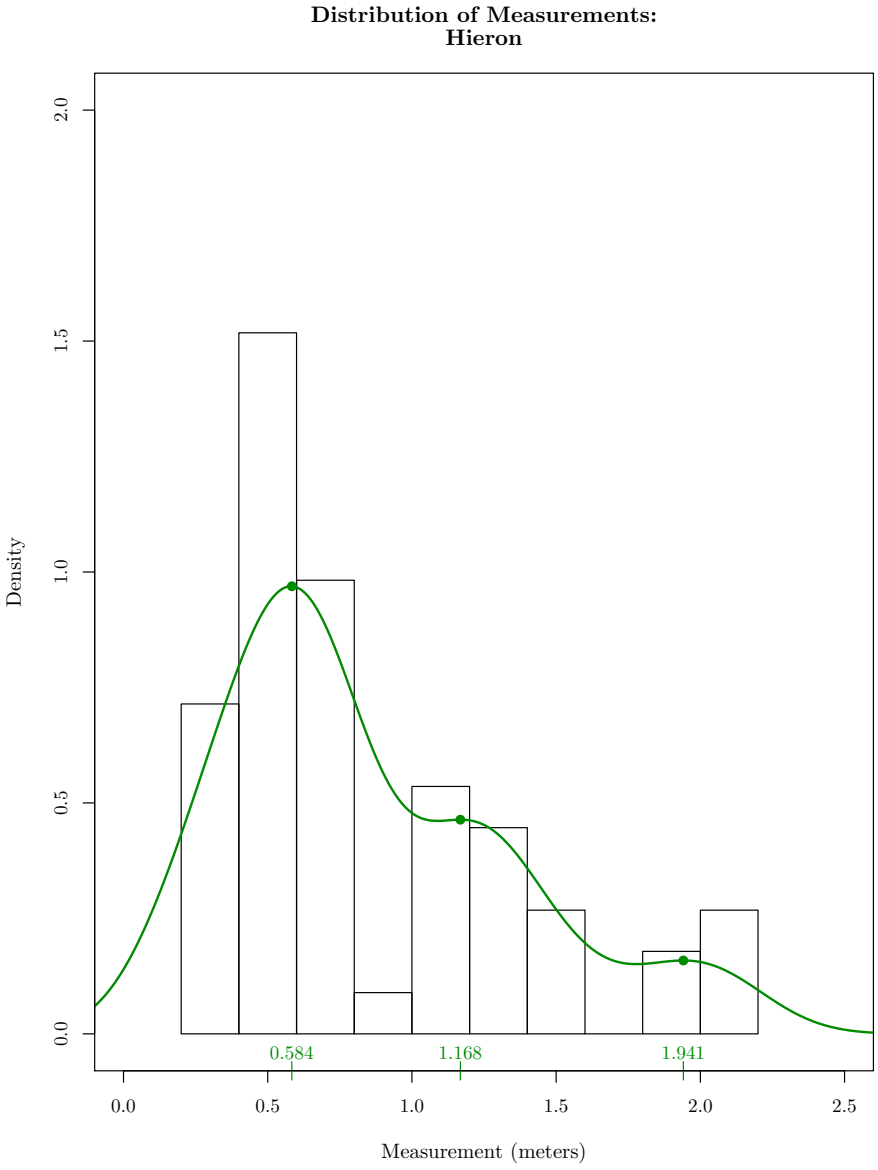

Figure 3: Histogram and KDE Function of Measurements from the Hieron

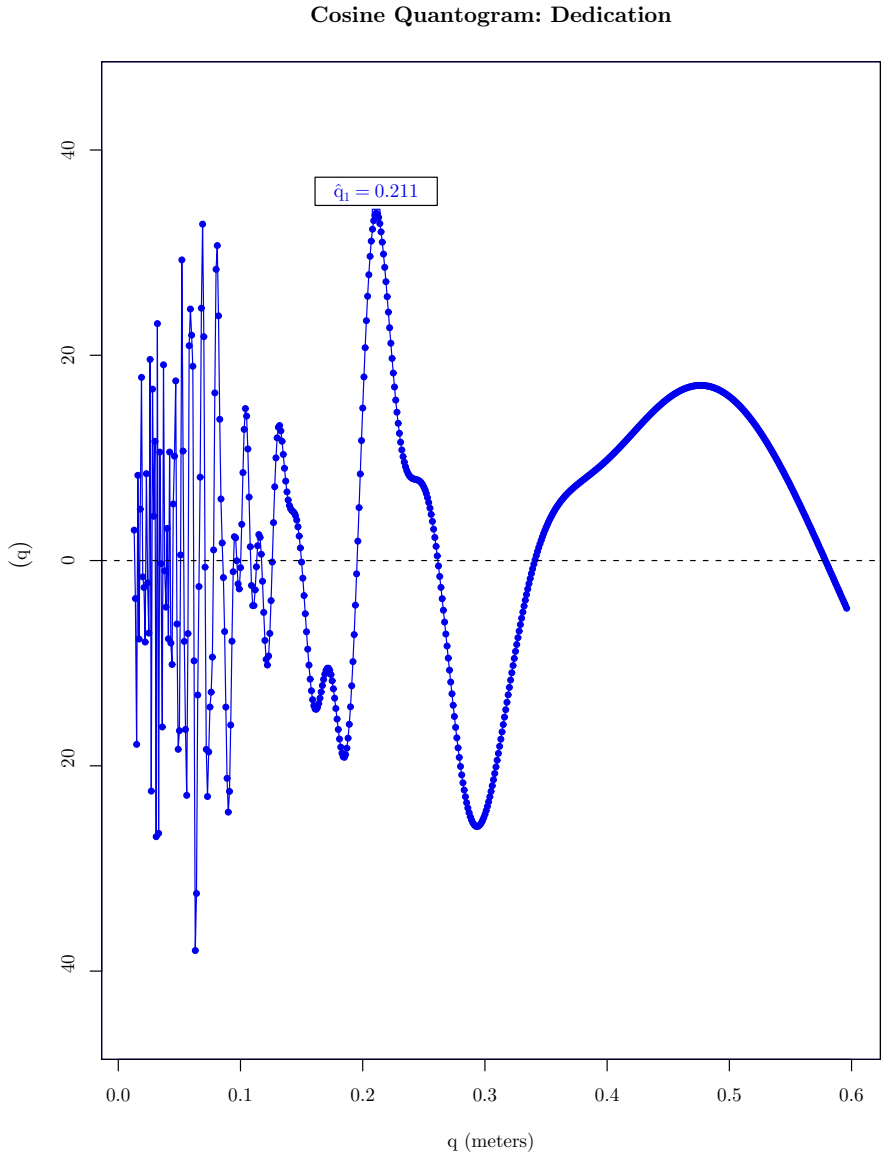

Figure 4: Cosine Quantogram Plot for Wall Blocks and Frieze Elements from the Dedication

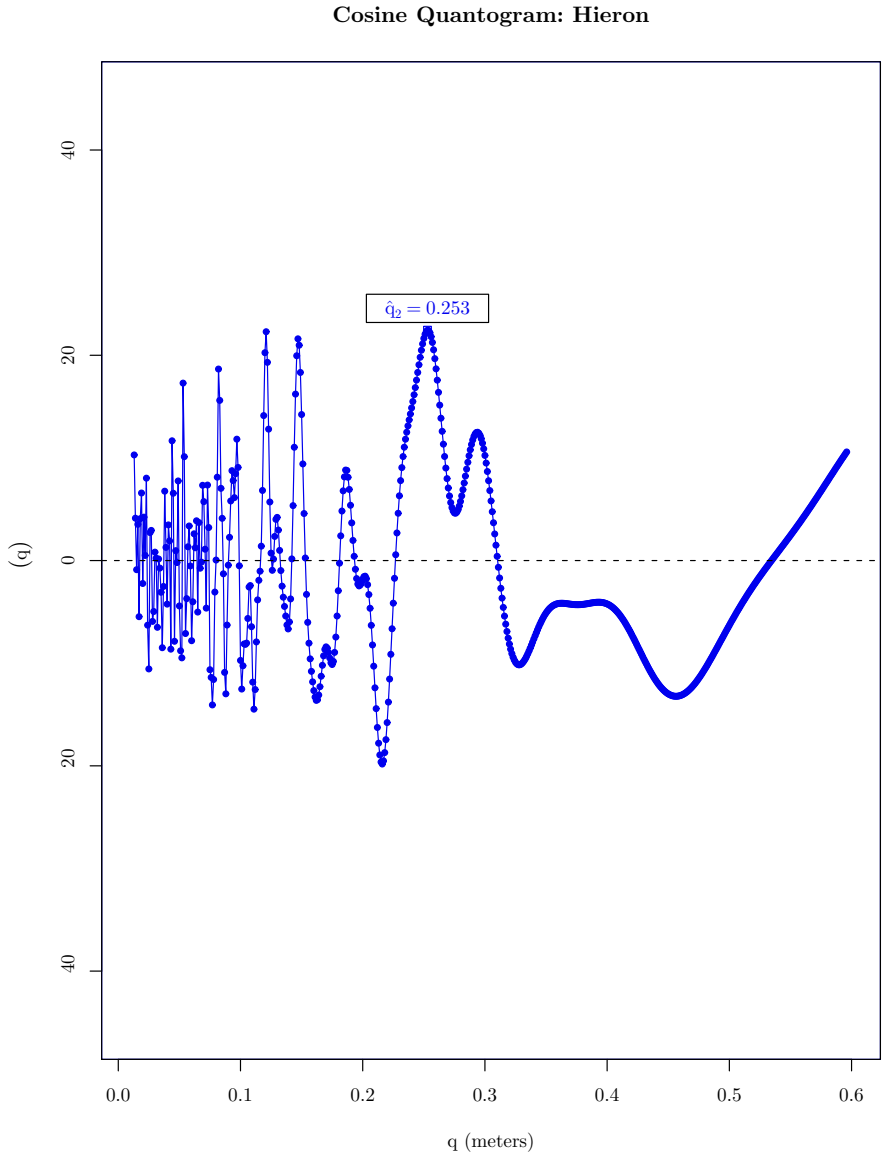

Figure 5: Cosine Quantogram Plot for Wall Blocks and Frieze Elements from the Hieron

3.4 Comparison of Quanta between Block Types within Buildings

3.4.1 Comparison of Quanta between Block Types of the Dedication

Figures 6 and 7 show the bimodal and multimodal distributions of the wall blocks and frieze elements of the Dedication, respectively. The modes of the distribution of the wall blocks occur at 0.444 meters and 1.003 meters. The 0.444-meter peak corresponds height measurements and the 1.003-meter peak corresponds to lengths. The modes of the frieze elements occur at 0.414 meters, 0.653 meters, and 1.043 meters, which represent the triglyph lengths, metope lengths and all heights, and frieze unit lengths, respectively.

In the Dedication, the estimate of the quantum for wall blocks is $\hat{q}_{11} = 0.255$ meters ($SE = 0.0718$ meters, 95% CI: (0.114 m., 0.396 m.)) and the quantum for frieze elements is $\hat{q}_{12} = 0.210$ meters ($SE = 0.0704$ meters, 95% CI: 0.072 m., 0.348 m.). These results are summarized in Table 8. The test statistic T_2 for the hypothesis that the quanta for the two block types within the Dedication are equal to the quantum for all blocks in the Dedication is -11.0078. There is not enough evidence to suggest that $q_{1\cdot} \neq q_{1j}$ for at least one block type j ($p = 0.645$). However, these quanta are vastly different in architectural terms. Figures 8 and 9 are plots of the cosine quantogram for the wall blocks and frieze elements, respectively.

Table 8: Comparison of Quanta between Wall Blocks and Frieze Elements of the Dedication

Block Type	$\hat{q}$	$SE(\hat{q})$	**95% Confidence Interval**
Wall Blocks	0.255	0.0718	(0.114, 0.396)
Frieze Elements	0.210	0.0704	(0.072, 0.348)

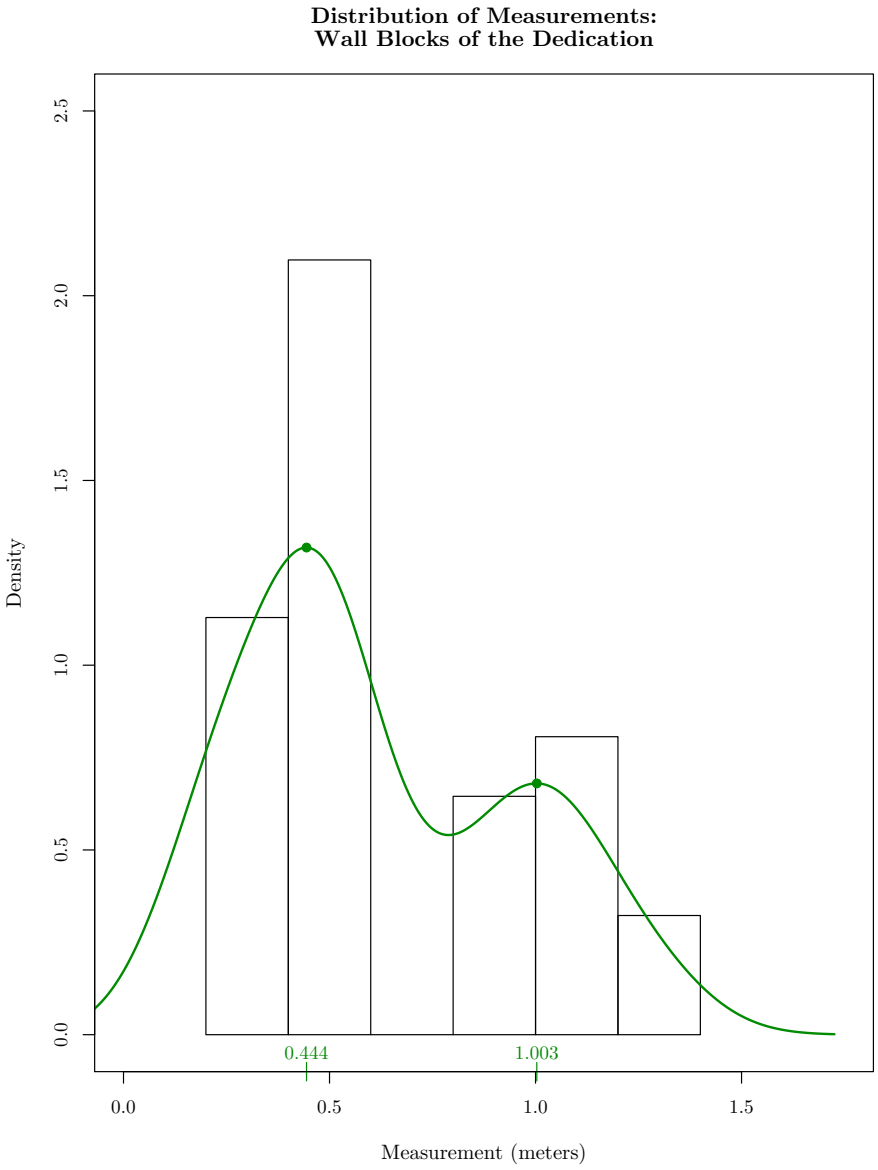

Figure 6: Histogram and KDE Function of Wall Blocks Measurements from the Dedication

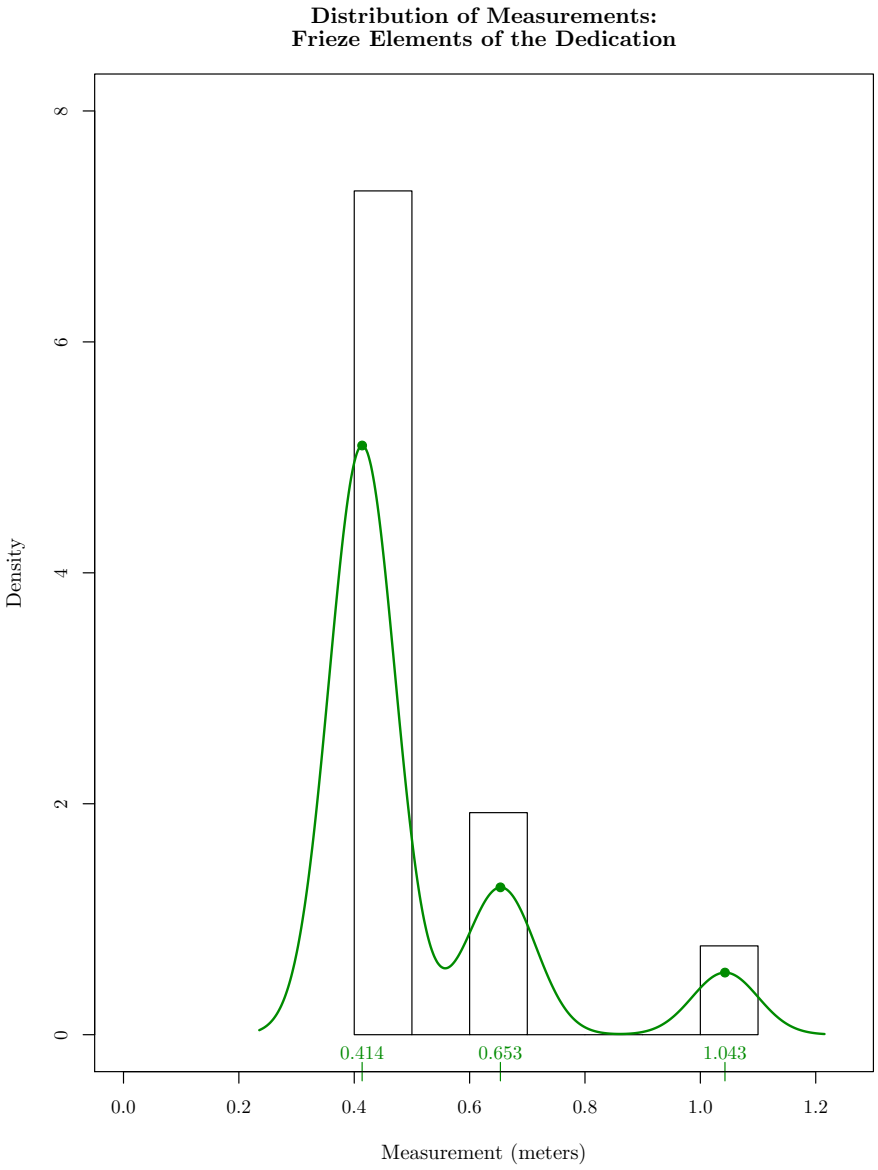

Figure 7: Histogram and KDE Function of Frieze Element Measurements from the Dedication

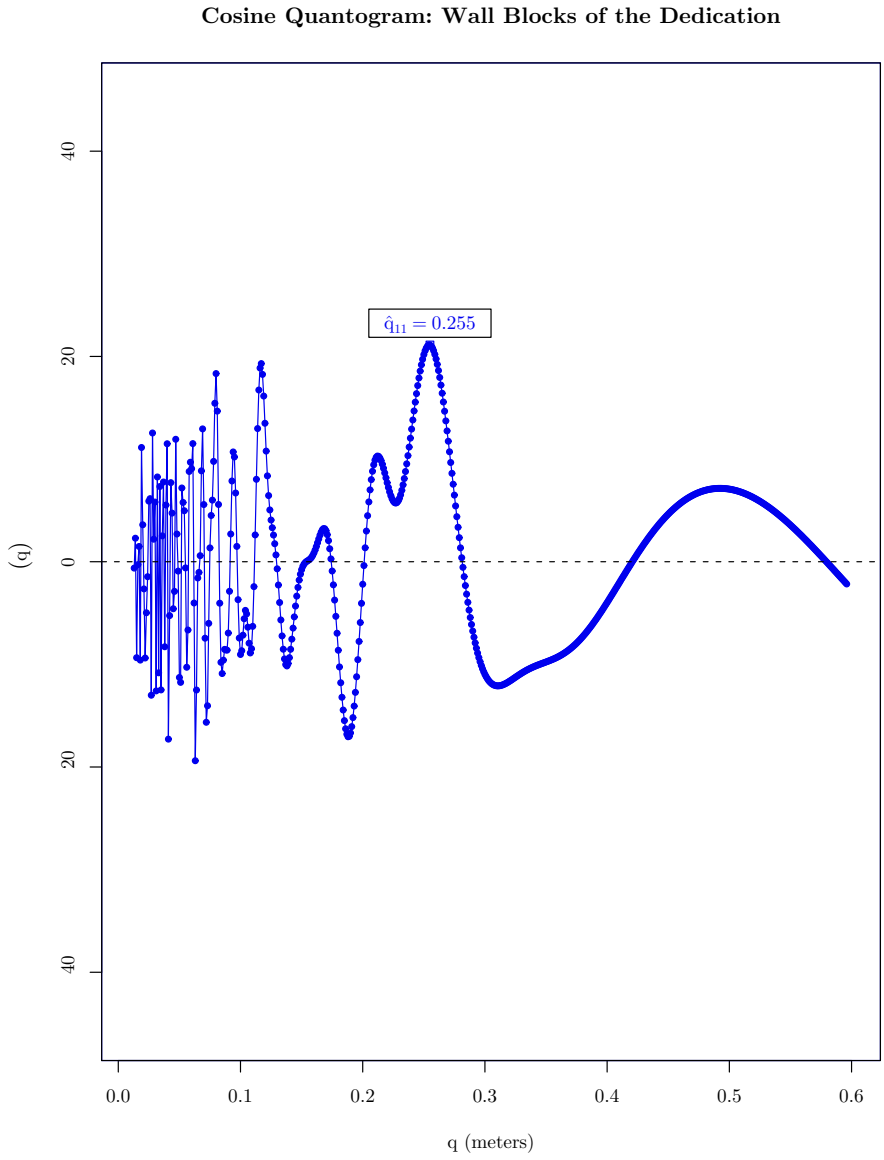

Figure 8: Cosine Quantogram Plot for Wall Blocks from the Dedication

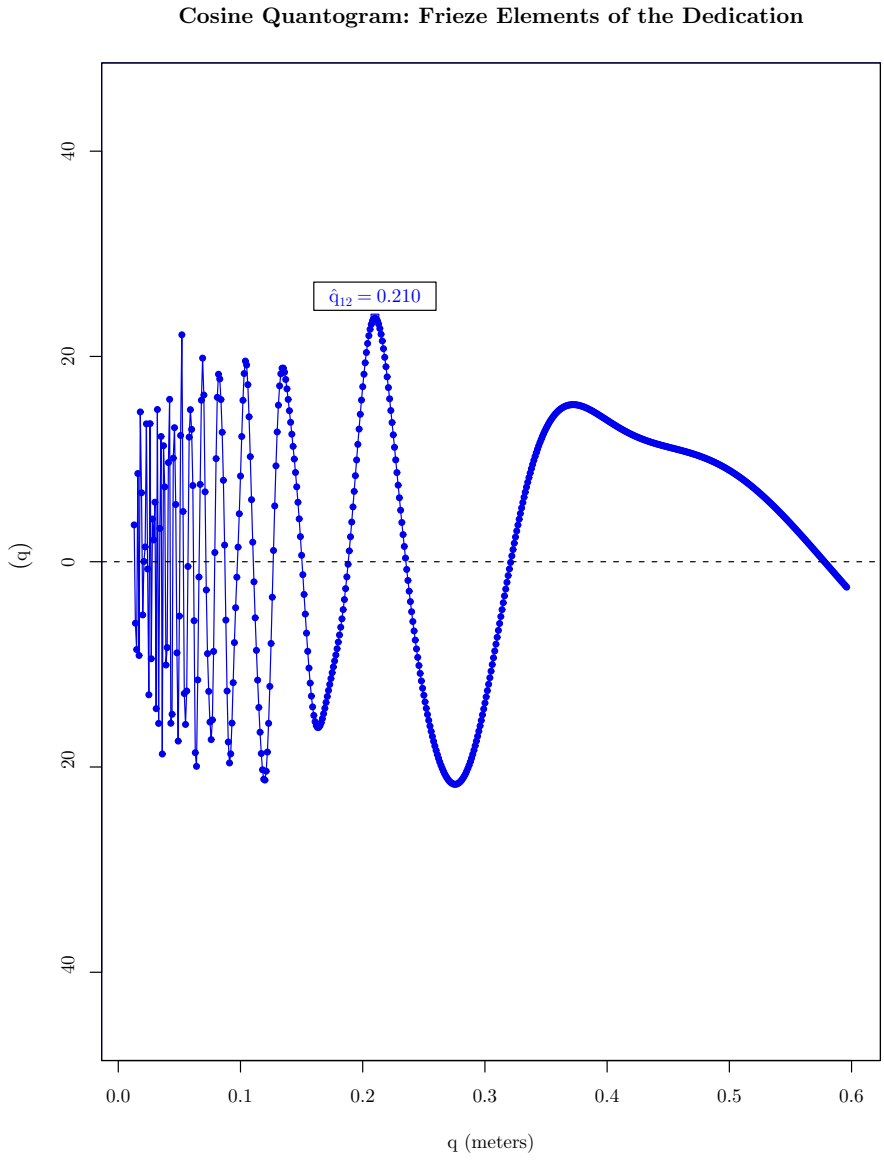

Figure 9: Cosine Quantogram Plot for Frieze Elements from the Dedication

3.4.2 Comparison of Quanta between Block Types of the Hieron

The distributions of the measurements for Hieron wall blocks and frieze elements are shown in Figures 10 and 11. In Figure 10, modes occur at 0.501 meters and 1.214 meters, which correspond to heights and lengths of wall blocks, respectively. The distribution of frieze elements in the Hieron (Figure 11) has peaks at 0.516 meters, 0.730 meters, and 1.205 meters, which are not evenly-spaced. The distance between the peaks at 0.730 meters and 1.205 meters is between 3 and 4 times the distance between 0.730 meters and 0.516, which does not suggest that there is a quantum for these data. However, the sample size may be too small ($n_{22} = 17$) to draw an accurate conclusion based on evenly-spaced modes of the absence of a quantum.

The estimate of the quantum for wall blocks of the Hieron is $\hat{q}_{21} = 0.295$ meters ($SE = 0.0693$ m., Figure 12). The estimate of the quantum for frieze elements in the same building is $\hat{q}_{22} = 0.244$ meters ($SE = 0.0150$ m., Figure 13). A 95% confidence interval for wall blocks is (0.159 m., 0.431 m.) and a 95% confidence interval for frieze elements is (0.241 m., 0.247 m.) (Table 9). The test statistic T_3 for the hypothesis that the quanta for the two block types are equal to the quantum for all blocks in the Hieron is -15.9371. There is not enough evidence to suggest that $q_{2\cdot} \neq q_{2j}$ for at least one block type j ($p = 0.810$).

Table 9: Comparison of Quanta between Wall Blocks and Frieze Elements of the Hieron

Block Type	$\hat{q}$	$SE(\hat{q})$	**95% Confidence Interval**
Wall Blocks	0.295	0.0693	(0.159, 0.431)
Frieze Elements	0.244	0.0015	(0.241, 0.247)

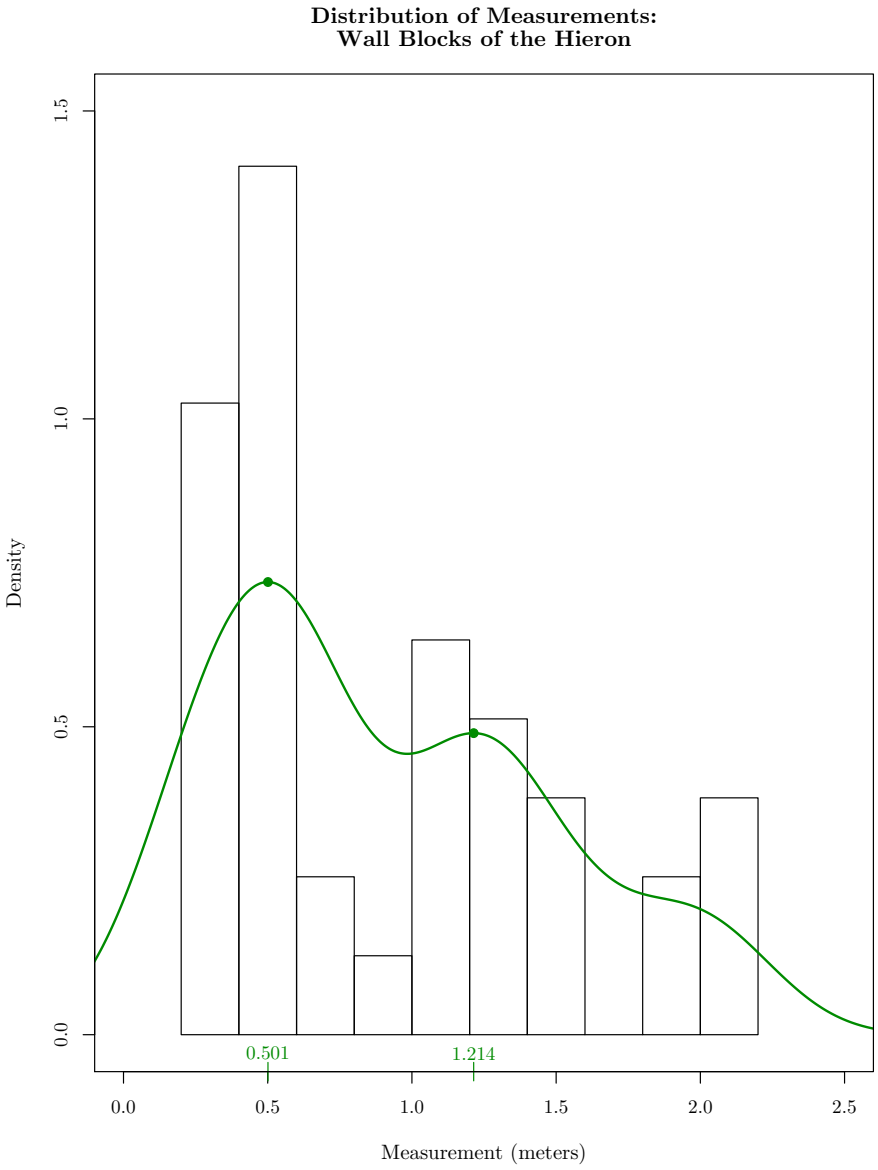

Figure 10: Histogram and KDE Function of Wall Block Measurements from the Hieron

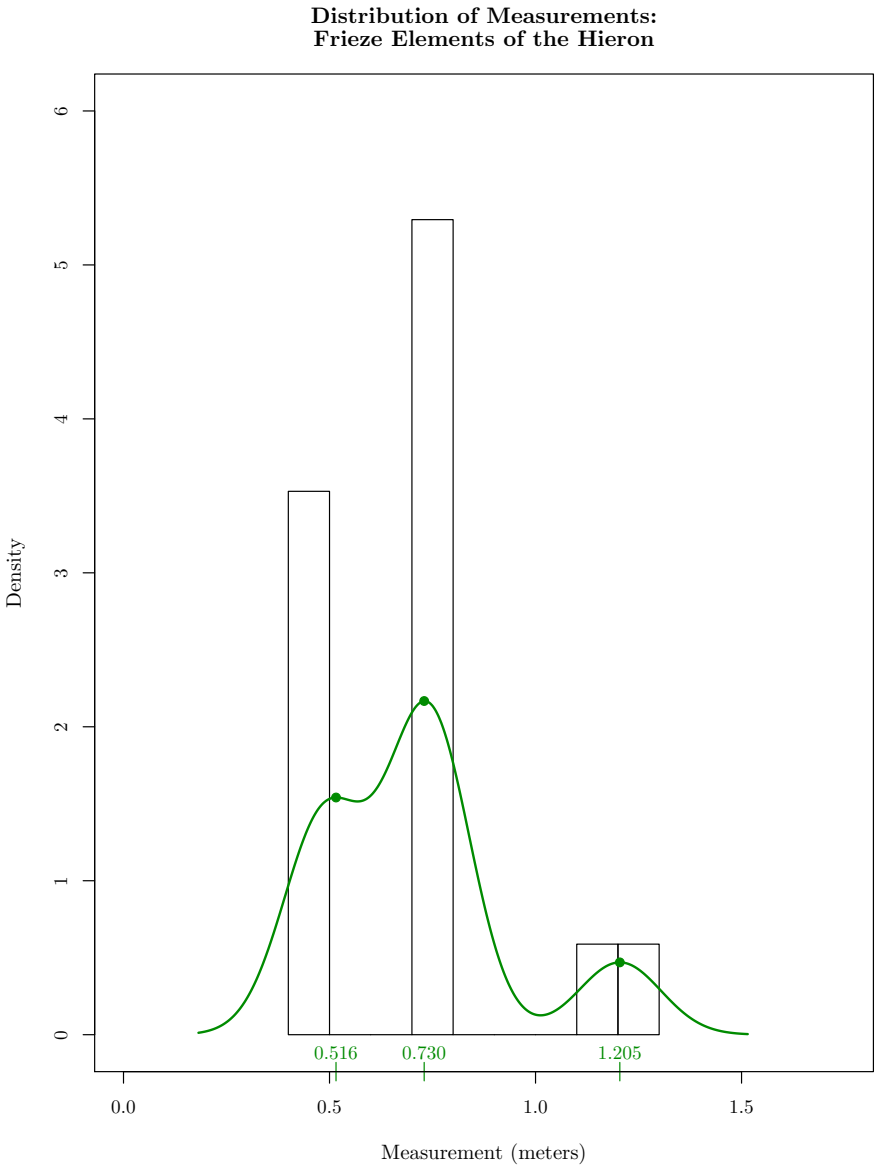

Figure 11: Histogram and KDE Function of Frieze Element Measurements from the Hieron

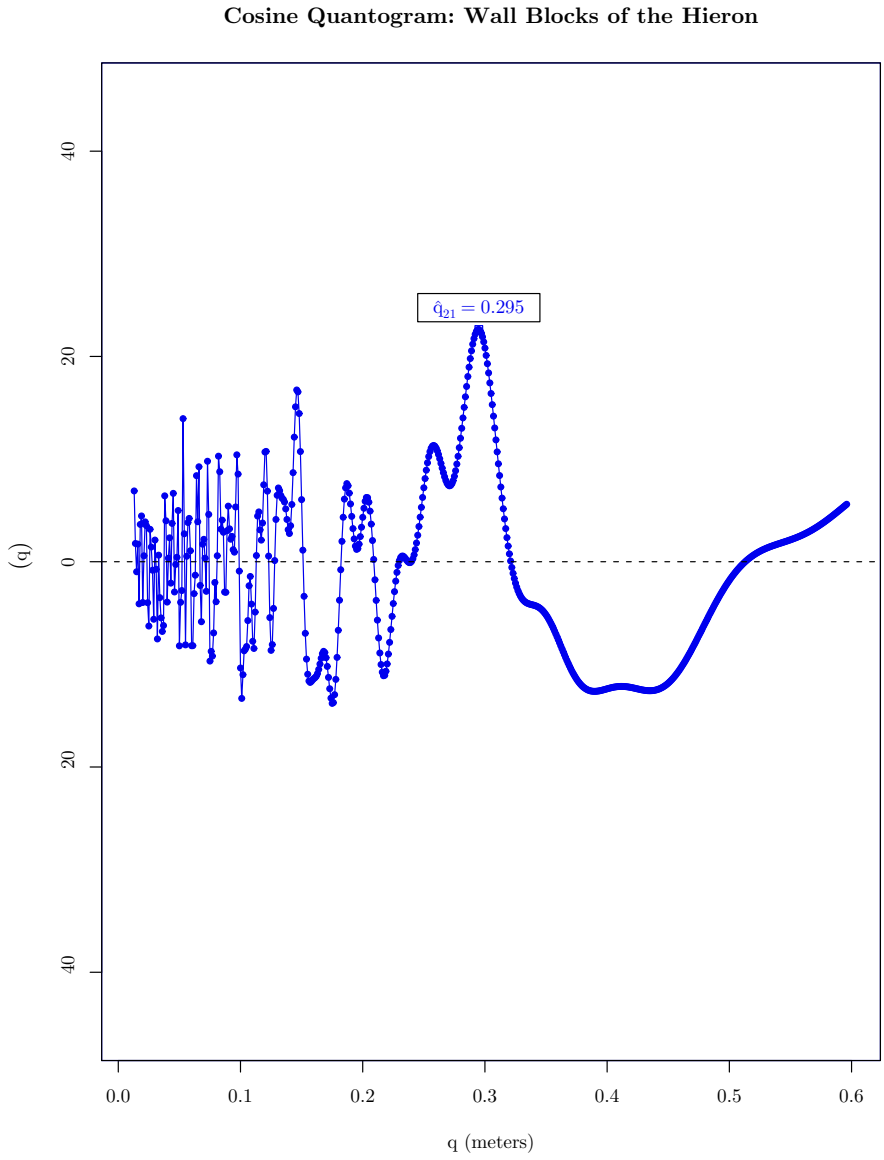

Figure 12: Cosine Quantogram Plot for Wall Blocks from the Hieron

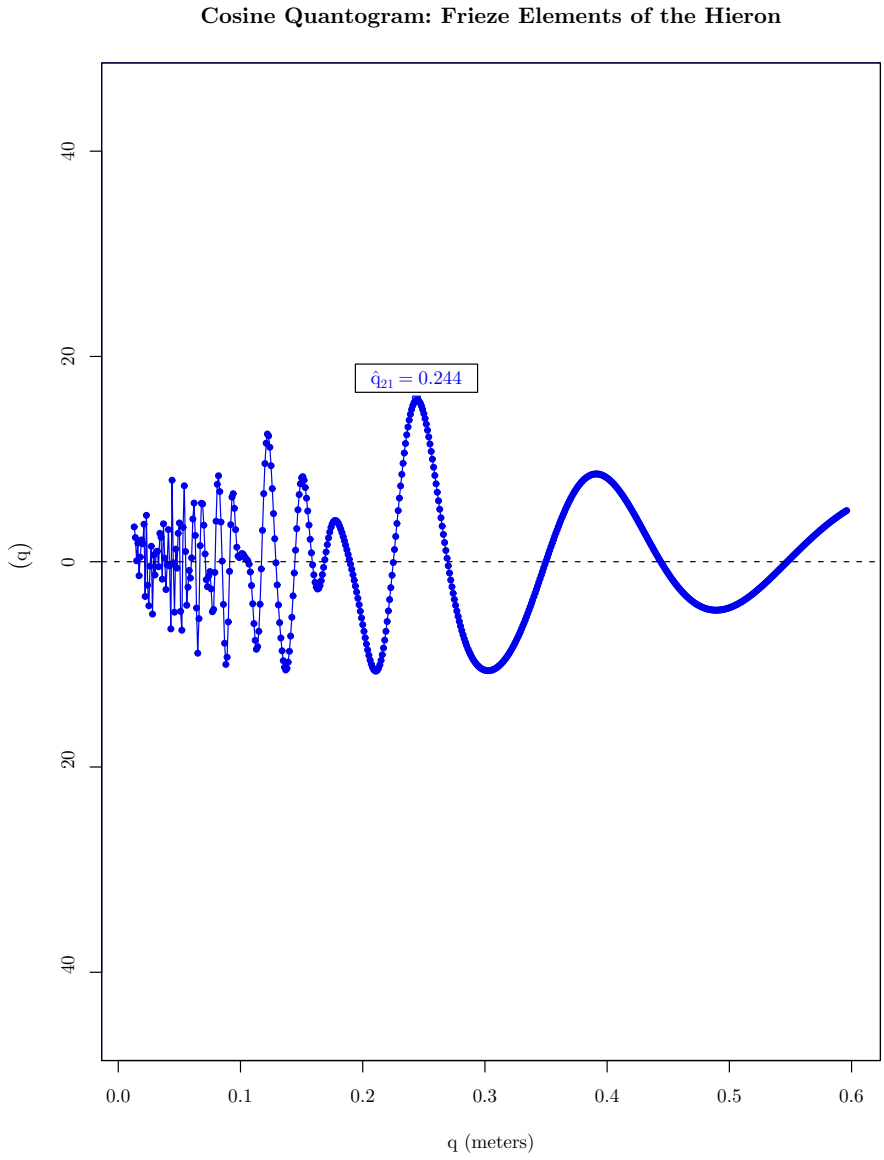

Figure 13: Cosine Quantogram Plot for Frieze Elements from the Hieron

3.5 Diagnostics

3.5.1 Goodness-of-Fit Tests

For the Dedication, the estimated von Mises distribution under the assumption that the circle's circumference is $\hat{q}_{1\cdot} = 0.211$ meters is $VM(0.214, 1.541)$ where $\hat{\mu}_{1\cdot} = 0.214$ radians is the maximum likelihood estimate of the mean direction and $\hat{\kappa}_{1\cdot} = 1.541$ is the MLE of the concentration parameter. Watson's test indicates that this von Mises distribution does not fit the data well ($U^2_{1\cdot} = 0.4797$, critical value = 0.092). This lack of fit suggests 0.211 meters may not be a good estimate of the quantum. For the Hieron, the estimated von Mises distribution under the assumption that the circle's circumference is $\hat{q}_{2\cdot} = 0.253$ meters is $VM(0.055, 0.876)$. This von Mises distribution does fit the measurements from the Hieron well ($U^2_{2\cdot} = 0.0476$, critical value = 0.079). Figures 14 and 15 show the distributions of errors for the Dedication and the Hieron, respectively. The red line shows the MLE of μ and the value is of $\hat{\mu}$ labeled in red.

3.5.2 Significance Testing for the Mean Direction Parameter, μ

For the Dedication, the MLE of the mean direction parameter μ of the assumed von Mises distribution formed around a circle of circumference equal to $\hat{q}_{1\cdot} = 0.211$ meters is $\hat{\mu}_{1\cdot} = 0.214$ radians ($SE = 0.1371$). The MLE of the concentration parameter κ is $\hat{\kappa}_{1\cdot} = 1.541$ ($SE = 0.2707$). Using 10,000 replicates, a 95% bootstrap confidence interval for $\mu_{1\cdot}$ is (-0.04, 0.52) and for $\kappa_{1\cdot}$ is (1.09, 2.12). In the test to determine whether the mean direction is equal to zero, H_0 cannot be rejected at the $\alpha = 0.05$ level; there is not enough evidence to suggest that the mean direction is not equal to zero ($W = 2.305$, $p = 0.1290$).

For the Hieron, the von Mises distribution formed around a circle with circumference $\hat{q}_{2\cdot} = 0.253$ meters has a mean direction $\hat{\mu}_{2\cdot} = 0.055$ radians ($SE = 0.2255$) and

concentration parameter $\hat{\kappa}_{2\cdot} = 0.876$ ($SE = 0.2162$). A 95% bootstrap confidence interval for $\hat{\mu}_{2\cdot}$ is (-0.41, 0.53) and for $\hat{\kappa}_{2\cdot}$ is (0.52, 1.32). There is no significant difference between the mean direction from the distribution errors from the Hieron and zero ($W = 0.059$, $p = 0.8087$).

Within the Dedication, the MLE of the mean direction parameter μ_{11} of the assumed von Mises distribution formed around a circle of circumference equal to $\hat{q}_{11} = 0.255$ meters for wall blocks is $\hat{\mu}_{11} = -0.259$ radians ($SE = 0.1501$) and the MLE of the concentration parameter κ_{11} is $\hat{\kappa}_{11} = 2.035$ ($SE = 0.4496$). Using 10,000 replicates, a 95% bootstrap confidence interval for μ_{11} is (-0.53 m., 0.09 m.) and for $\hat{\kappa}_{11}$ is (1.40 m., 3.01 m.). There is not enough evidence to suggest that the mean direction is not equal to zero ($W = 0.009$, $p = 0.9257$). The von Mises distribution formed around a circle with circumference $\hat{q}_{12} = 0.210$ meters for frieze elements in the Dedication has a mean direction $\hat{\mu}_{12} = -0.046$ radians ($SE = 0.0830$) and concentration parameter $\hat{\kappa}_{12} = 6.111$ ($SE = 1.6050$). A 95% bootstrap confidence interval for μ_{12} is (-0.17, 0.13) and for κ_{12} is (3.39, 35.83). There is no statistically significant difference between the mean direction from the distribution of errors from Dedication frieze elements and zero ($W = 0.001$, $p = 0.9751$).

Within the Hieron, the MLE of the mean direction parameter μ_{21} of the assumed von Mises distribution formed around a circle of circumference $\hat{q}_{21} = 0.295$ meters (wall blocks) is $\hat{\mu}_{21} = -0.282$ radians ($SE = 0.1670$) and the MLE of the concentration parameter κ_{21} is $\hat{\kappa}_{21} = 1.526$ ($SE = 0.3253$). Using 10,000 replicates, a 95% bootstrap confidence interval for μ_{21} is (-0.54, 0.00) and for κ_{21} is (0.86, 2.72). In the test to determine whether the mean direction is equal to zero, we cannot reject H_0 at the $\alpha = 0.05$ level and conclude that the mean direction is equal to zero ($W = 2.647$, $p = 0.1037$). The von Mises distribution formed around a circle with circumference $\hat{q}_{22} = 0.244$ meters (Hieron frieze elements) has a mean direction of $\hat{\mu}_{22} = 0.051$ radi-

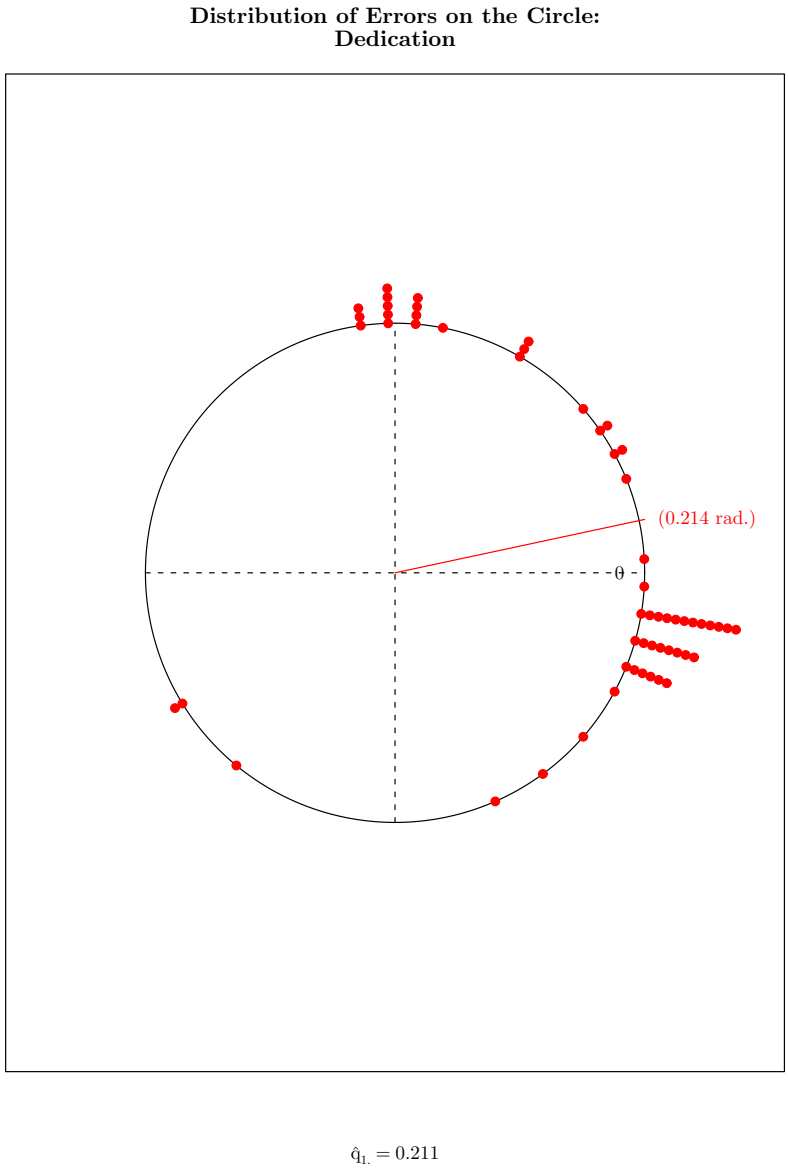

Figure 14: Distribution of Calculated Errors Assuming a Von Mises Distribution for Measurements from the Dedication

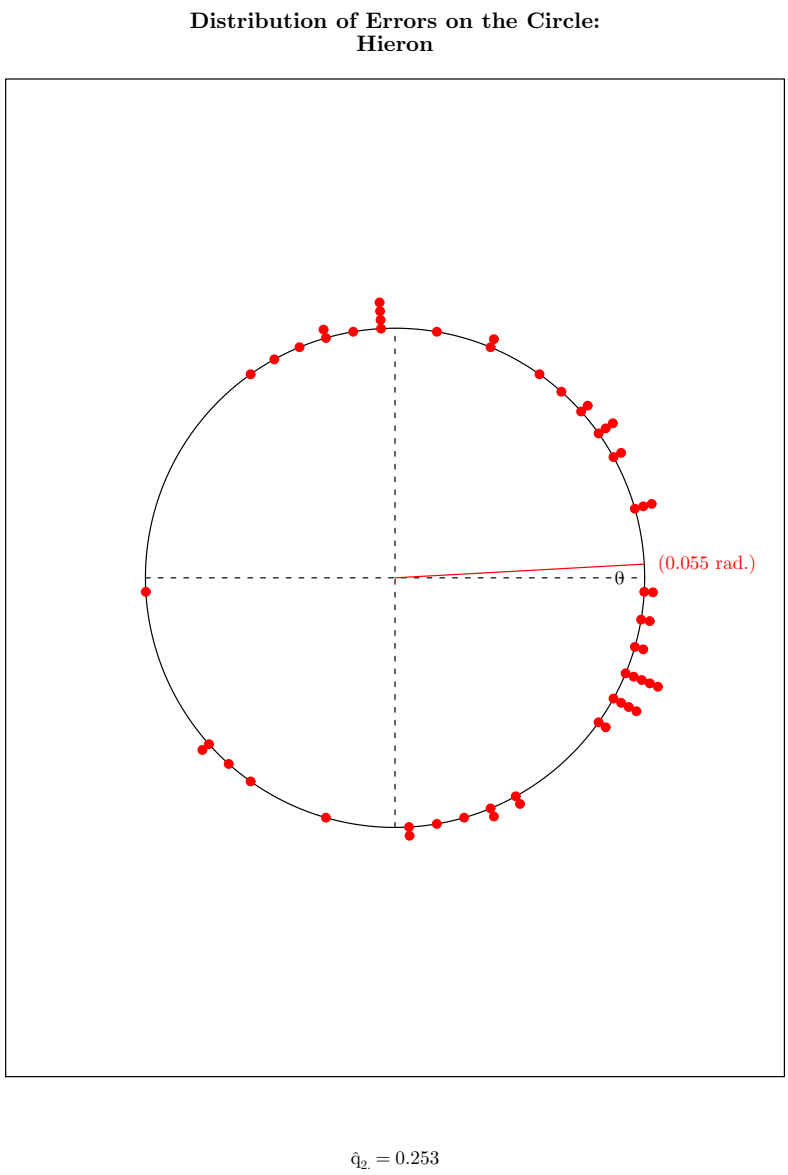

Figure 15: Distribution of Calculated Errors Assuming a Von Mises Distribution for Measurements from the Hieron

ans ($SE = 0.0937$) and a concentration parameter of $\hat{\kappa}_{22} = 7.222$ ($SE = 2.3720$). A 95% bootstrap confidence interval for μ_{22} is (-0.14, 0.23) and for κ_{22} is (4.59, 15.03). There is no statistically significant difference between the mean direction from the distribution of errors from Hieron frieze elements and zero ($W = 0.002$, $p = 0.9624$).

3.5.3 Two-Sample Tests of Homogeneity

In the tests of homogeneity of distributions, the $\alpha = 0.05$ level critical value against which the test statistics are compared is 0.187. For the comparison between blocks in the Dedication and blocks of the Hieron the test statistic is 0.314; there is a statistically significant difference between the distributions of the Dedication and Hieron measurements. For the test of homogeneity in wall blocks and frieze elements within the Dedication, the test statistic is 0.8372; there is a statistically significant difference between the distributions of the wall block and frieze element measurements within the Dedication. Similarly, when comparing the distributions between wall block and frieze elements in the Hieron, the test statistic is 0.3118; there is a statistically significant difference between the distributions of the wall block and frieze element measurements within the Hieron. Rejecting the null hypothesis that the measurements come from the same distribution in all cases indicates that the measurements (and errors) in pairs of subgroups come from different populations.

4 Discussion

4.1 Art Historical Implications of the Calculated Quanta

The relevance of a quantum calculated at the micro-dimensional level (i.e., from individual block measurements) relies on how the unit is used at the macro-dimensional level. The macro-dimensional level consists of larger measurements such as length and width of the building at the stylobate level, length of the frieze, and interaxial space between columns. It also includes 'ideal' measurements of smaller components, such as triglyph and metope lengths, which are generally established by finding the median of unbroken measurements. An objective way to verify that a quantum fits a dimension well is to divide the measurement by the quantum, round the result to the nearest positive integer M to find the approximate number of quanta in the measurement, then divide the measurement M to find what the quantum should be, based on M. Because small errors build up quickly in larger dimensions, if the discrepancy d between the original proposed quantum and the new M-based quantum ($\tilde{q}$) is less than 0.001 meters, then the original quantum works well for that component. Furthermore, a quantum may be considered 'good' if M is divisible by 5 or by values that relate to 16, the number of dactyls in a cubit – namely 2, 4, 8, 16, 24, and 32.[4]

Cosine quantogram analysis yielded a quantum of 0.211 meters for the Dedication. Vertical measurements (heights) did not have $\tilde{q}$'s close to the estimate of the quantum (Table 10). The best fit of the quantum to a major component is with the interaxial space between columns, at $9\hat{q}_{1.}$ ($d = 0.0002$). This relationship puts the ratio between the quantum and the interaxial distance at 1:10, but with 0.0034 meters discrepancy. The quantum fits the stylobate width and the building width at the first step well ($d =$

[4] According to M. Wilson Jones (2001), "the appeal of multiples of 5 may be linked to the fact that this number is one of the bases of Greek counting systems" (p. 690).

Table 10: Use of a 0.211-meter and a 0.208-meter Quantum in the Dedication

Component	**Y (m.)**	M		$\tilde{q}$		$d = \lvert\hat{q} - \tilde{q}\rvert$	
		0.211	0.208	0.211	0.208	0.211	0.208
Axial Width of Façade	10.046	48		0.2093		0.0017	0.0013
Building Width at First Step	12.414	59	60	0.2104	0.2069	0.0006*	0.0011
Stylobate Width	11.011	52	53	0.2117	0.2077	0.0007*	0.0003*
Interaxial Distance at Corner	1.901	9		0.2112		0.0002*	0.0032
Interaxial Space of Columns	2.076	10		0.2076		0.0034	0.0004*
Lower Column Diameter	0.835	4		0.2088		0.0023	0.0008*
Upper Column Diameter	0.685	3		0.2283		0.0173	0.0203
Abacus Width	0.863	4		0.2158		0.0048	0.0078
Epistyle Width	0.755	4		0.1888		0.0223	0.0193
Metope Length	0.621	3		0.2070		0.0040	0.0001*
Stylobate Block Width	1.034	5		0.2068		0.0042	0.0012
Triglyph Length	0.416	2		0.2080		0.0030	0.0000*
Capital Height	0.333	2		0.1665		0.0445	0.0415
Column Height	5.450	26		0.2096		0.0014	0.0416
Entablature Height	1.442	7		0.2060		0.0050	0.0020
Epistyle Height	0.544	3		0.1813		0.0297	0.0153
Frieze Height	0.670	3		0.2233		0.0123	0.0200
Geison Height	0.228	1		0.2280		0.0170	0.0267
Krepis Height	0.791	4		0.1978		0.0133	0.0103

*sufficiently small d (< 0.001 m.)

0.0007 and 0.0006, respectively). However, the relationship between these dimensions and the quantum are not ideal and do not make sense: the stylobate width is $52\hat{q}_{1.}$ and the width of the building at the first step is $59\hat{q}_{1.}$. The large errors associated with the $10\hat{q}_{1.}$ interaxial distance hypothesis raises the possibility of a quantum with high likelihood of being the quantum and with small errors (d) associated with both the micro- and macro-dimension levels.

An interesting dilemma arises if we consider the quantum for the Dedication to be half the length of an average triglyph (0.416 meters),[5] or $\hat{q}_{1.} = 0.208$ meters. Based on the number of best-fitting dimensions, a quantum of 0.208 meters fits the principal façade dimensions better than the 0.211-meter quantum found using the cosine quantogram method (Table 10). The positive integer multiple, M, of each quantum is the same for all dimensions except the building width at the first step and the stylobate width. If the quantum is indeed 0.208 meters, then the interaxial distance between columns is almost exactly $10\hat{q}_{1.}$ ($d = 0.0004$). The positive integer multiple of the 0.208-quantum for building width at first step becomes a more favorable $60\hat{q}_{1.}$, but at the cost of a large d. It should also be noted that the next highest peak in Figure 4 occurs at $q = 0.069$, or a little less than one third of 0.208 meters. Furthermore, $q = 0.104$ meters, one half of 0.208 meters, is also a local maximum.

The two possible values for $\hat{q}_{1.}$, 0.211 meters and 0.208 meters, appear to be equivalent in terms of errors produced when they are fitted against the micro-level components (Table 11). From Table 10 there is no statistically significant difference between the paired discrepancies calculated from the proposed quanta $\hat{q}$ and their corresponding M-based quanta $\tilde{q}$ (Wilcoxon signed-rank test p-value = 0.2398). The

[5]The median triglyph length was calculated to be 0.415 meters based on the lengths of actual triglyphs and whole mutules and regulae. However, halves of mutules and regulae may be present on geison blocks and epistyle blocks, respectively. These portions may be matched to others in the dataset. For simplicity, these were not included in the cosine quantogram analysis. However, the average of 0.416 meters comes from the inclusion of these other lengths.

next step in this dilemma is to construct a test for the simple null hypothesis that $q_{1\cdot} = 0.208$ and the composite alternative that $q_{1\cdot} \neq 0.208$. This test may be constructed using a log-likelihood ratio test and bootstrapping as before to determine where in the distribution of $\hat{\phi}^*(0.208)$ the estimate $\hat{\phi}(0.208)$ lies. If the result of this test is not statistically significant (i.e., we conclude that $q_{1\cdot}$ may be 0.208 meters), then we can test if 0.208 and 0.211 are statistically significantly different from each other with the simple null hypothesis that $q_{1\cdot} = 0.211$ versus the simple alternative that $q_{1\cdot} = 0.208$.

Table 11: Summary of Errors Produced with a 0.208-meter and a 0.211-meter Quantum in the Dedication

Quantum (m.)	**Mean (SD)**	**SE**	**Median**	**Min.**	**Max.**	**Range**
0.208	0.0244 (0.0259)	0.0034	0.0100	0.0000	0.0780	0.0780
0.211	0.0263 (0.0229)	0.0030	0.0150	0.0010	0.0870	0.0860

At first glance, the quantum of 0.253 meters for the Hieron does not fit the smaller architectural elements such as the capital height, epistyle height, diameters of columns, interaxial space between columns, etc. (Table 12). The quantum performed well for the triglyph and metope lengths. However, the larger building dimensions such as length and width at the stylobate, length of frieze, etc. are remarkable. For a couple of dimensions, M is a multiple of five, with very small discrepancy. Both of these dimensions pertain to the stylobate level – the length and the width of the building at the level stylobate. The length of the building appears to be equal to $155\hat{q}_{2\cdot}$ and the width is exactly $50\hat{q}_{2\cdot}$. If the 0.253-meter quantum is correct, then it suggests that the Hieron was designed with the overall dimensions in mind.

For the within buildings tests, it was determined that the quantum for wall blocks within the Dedication (q_{11}) and the quantum for frieze elements of the Dedication (q_{12}) were equal. This was also true in the Hieron; it was concluded that $q_{21} = q_{22}$. However, to an archaeologist, there is a large discrepancy between appropriate pairs

Table 12: Use of a 0.253-meter Quantum in the Hieron

Component	**Y (m.)**	M	$\tilde{q}$	$d = \lvert\hat{q} - \tilde{q}\rvert$
Building Width at First Step	14.03	55	0.2551	0.0021
Euthynteria Width	12.79	51	0.2508	0.0022
Stylobate Length	39.25	155	0.2532	0.0002*
Stylobate Width	12.65	50	0.2530	0.0000*
Interaxial Distance at Corner	2.18	9	0.2422	0.0108
Interaxial Space of Columns	2.39	9	0.2656	0.0278
Lower Column Diameter	0.901	4	0.2253	0.0278
Upper Column Diameter	0.783	3	0.2610	0.0080
Abacus Width	1.021	4	0.2553	0.0023
Epistyle Width	0.86	3	0.2867	0.0337
Metope Length	0.72	3	0.2400	0.0013
Triglyph Length	0.48	2	0.2400	0.0013
Capital Height	0.41	2	0.2050	0.0480
Column Height	5.66	22	0.2573	0.0043
Entablature Height	1.607	6	0.2678	0.0148
Epistyle Height	0.637	3	0.2123	0.0407
Frieze Height	0.745	3	0.2483	0.0047
Geison Height	0.225	1	0.2250	0.0280

*sufficiently small d (< 0.001 m.)

of point estimates. Ancient Greek buildings were constructed with small errors on a scale of millimeters, even for large dimensions. The difference between $\hat{q}_{11} = 0.255$ and $\hat{q}_{12} = 0.210$ is 0.045 meters. The difference between $\hat{q}_{21} = 0.295$ and $\hat{q}_{22} = 0.244$ is 0.051 meters. Archaeologists assume that the quanta for block types within building are the same, with the possible allowance of a few millimeters variation. This conflict can be resolved by deriving a new hypothesis testing procedure that has more power – the probability that we reject a false null hypothesis (i.e., we conclude that the quanta are not equal given that quanta are actually not equal).

4.2 Sources of Error in Block Dimensions

All blocks of the same type should have exactly the same measurements with no variance. Error occurs when the measured dimension of a block is different than the ideal value. There are several possible sources of error when dealing with measurements. First, there is human error during the measuring phase, which includes, but is not limited to, rounding error. An obvious source of error is erosion. This source, however, is minimal because block surfaces were smoothed to allow for smooth exterior and interior walls, as well as seamless joints between adjacent blocks and these surfaces have been preserved. The method of measurement accounts for it as much as possible.

The largest source of potential error is the conflict between the building as designed and the building as constructed. Assuming there was a building plan prior to construction, the number and dimensions of every block imported from off-site would have to be known prior to sending the block orders to the quarry. In addition, to prevent block dimension loss during transport, blocks would have been cut larger at the quarry and cut smaller on-site. If a block used was too long, in order to compensate, another block would have to be cut smaller than its original design. The dimension

most affected by this type of error is length. Height was probably a stable dimension, because height needed to be consistent for the roof to be level.

Although Greek architecture aimed at mathematical harmony, it was nonetheless problematic. The Doric corner conflict arises when a triglyph must line up with the corners of the frieze. Because columns must also support the corners of the structure, the conflict occurs when the middle of the triglyph does not line up with the middle of the corresponding column. One solution to this, which could affect the outcome of analysis, is to adjust the length of the corner triglyphs so that the middle extends to the middle of the corner column (Coulton, 1977). However, by the Hellenistic period, architects were able to project dimensions downward from a uniform frieze.

Any errors produced by any of these sources are accounted for in this study. First, any modern measurement error should be minimized with the unrounding procedure used. Errors produced by ancient measurement error are accounted for in the confidence intervals. However, if we knew the location in the façade of all the blocks, we could determine and model the errors in heights. Length errors would be more difficult to model because it is the most variable.

4.3 Limitations of Previous Studies

In each study involving the cosine quantogram method by Kendall and Pakkanen, the only inference conducted involved testing the existence of a quantum, but no focus is given to determining confidence intervals for the quantum or testing the equality of quanta between groups of data. The confidence interval is as important as the point estimate $\hat{q}$ because it accounts for other possible samples from the population of measurements. Significance testing provides a way to test if a quantum from one building of unknown quantum is equal to the quantum from a another building (or buildings) of known quantum (quanta). Not utilizing other types of statistical inference besides

point estimation limits the ability to arrive at meaningful conclusions.

4.4 Limitations of This Study

One limitation of this method of calculating the quantum is that it does not take into account a correlation between the height, length, and width of each block. These measurements have been assumed to be independent. This naïve approach to the problem is not detrimental to calculating an accurate quantum, but the more information about the source of the measurements that is incorporated into the method, the more meaningful the conclusion.

It appears in the literature that there have been no attempts to test the validity of the cosine quantogram method. A way to test the validity would be to simulate data where the data are forced to have a predefined quantum. Since a quantum exists and is known, 10,000 samples from the distribution could be generated. The cosine quantogram method is then applied to each sample. The mean and standard error of the calculated quanta could be calculated and a confidence interval could be constructed.

Another issue with the cosine quantogram method is that often a integer multiple of the quantum plus a fraction of the quantum will fit one of the macro-dimension measurements well. By definition, this subdivision of the quantum cannot happen; it is the smallest unit present in the data. This issue raises the question of whether a subdivision of the proposed quantum could be the true quantum instead? A subdivision of the quantum fits the definition that it is a unit that cannot be subdivided further and that each measurement can be expressed as a positive integer multiple of the quantum. However, the cosine quantogram equation describes the likelihood that a value of q is the true quantum; the higher the value of $\phi(\cdot)$, the more likely that value of q is the quantum. In the cosine quantogram plot of the Dedication, it was

apparent that divisors of 0.208, which was not the abscissa of the maximum of $\phi(\cdot)$, had higher likelihoods of being the quantum than other q's around them. It appears that the cosine quantogram method is similar to other statistical methods, such as model selection in regression analysis, in that it is steeped in objective mathematical theory, but in the end, choosing a quantum also has a subjective component.

4.5 Biological Applications

Newson, Parker, and Barlow (1993) used the cosine quantogram method to determine if the distances between lateral roots of the *Lycopersicon esculentum* Miller species of tomato plant were multiples of a quantum measurement. Lateral, or secondary, roots extend horizontally from the primary root, which extends vertically into the ground. From inspection of the distribution of the distances, there appeared to be a multimodal distribution with modes occurring at fixed distances. The existence of a quantum from these data would provide insight into growth and cell differentiation mechanisms in the tomato plant. However, in general, the data presented by Newson, et al. did not exhibit a quantal relationship.

The cosine quantogram method may be applied to study any periodic biological phenomenon. One such application in phenology is to study the effects of global warming. Because temperature data may not exist in some regions and some time periods, temperature-dependent animal and plant life cycles may be used as surrogate indicators of temperature. Departures from a quantal relationship between time and onset of a phenomenon, such as germination or bird migration, could indicate a climate change effect.

4.6 Public Health Implications

Thaler and Braun (1984) applied the cosine quantogram method to determine if albumin production in clonal cells is clustered around values of the geometric sequence of the form $a_n = c\left(\sqrt{(2)}\right)^n$. The null hypothesis that the i^{th} observation of activity level Y_i is equal to some constant c multiplied by a constant P raised to a positive integer M_i (i.e., $H_0 : y_i = aP^{M_i}$) may be log-transformed to be $\log(y_i) = \log(C) + M_i \log(P)$. The term $\log(C)$ may be omitted without loss of generality because only relative enzyme activities are considered. In this study, the quantum $q = \log(P)$ is equal to $\log(\sqrt{(2)})$. There was no evidence to suggest that $q = \log(\sqrt{(2)})$ is the quantum. Furthermore, no evidence of periodicity exists for any value of q related to $\sqrt{(2)}$, which is supported by the fact that higher peaks in the quantogram exist for values of q unrelated to $\sqrt{(2)}$, although a local maximum occurs at $q = \log(2) = 2\log(\sqrt{(2)})$. The authors conclude that albumin production in clonal cells is not clustered around a geometric sequence involving $\sqrt{(2)}$.

An important application of finding a quantum would be in morphometry. In the case of neuroimaging, voxel-based morphometry has been used to study differences in brain structure among patients in disorder populations (Ashburner & Friston, 2000). Quantal analysis is most pertinent to the issue of brain shape and the size of structures, but is not particularly useful for providing insight into the location of certain structures. Studying the quanta of brain structures in 'normal' patients could lead to a more accurate brain atlas for comparison with diseased brains and brains with physiological disorders.

4.7 Future Directions

The next step in analyzing the data from the Sanctuary of the Great Gods is to incorporate other Doric buildings from the site, such as the Stoa and the Rotunda of Arsinoe. Each building adds its own unique challenges to analysis. Recall that the Stoa was constructed using porous limestone blocks, which were then covered in plaster. It was not necessary to have precise measurements for each block dimension because the plaster concealed any imperfections. The Rotunda of Arsinoe is the largest circular structure in the Ancient Greek world. Because its blocks are curved, the measurements governed by the quantum may not be the dimensions of the surface area of the external face. The length could be the maximum length of the block or the arc length of the interior or the exterior face.

We assume that there is no difference in the quantum defined for heights, lengths, and widths within blocks and that there is no correlation between dimensions. The assumption that the quanta for heights, lengths, and widths are equal is reasonable because there is no evidence to suggest that there were different measuring rods for each dimension. However, the assumption that there is no correlation between dimensions within a block is naïve because the Ancient Greeks placed considerable emphasis on *symmetria*. Ratios between dimensions may be consistent and might resemble established ratios such as the golden ratio ($\phi \approx 1.61803$) or the silver ratio ($\delta_s = 1 + \sqrt{(}2) \approx 2.41421$). There should at least be some dependence relationship between height and length, because the aesthetics of the exterior and interior block faces would be most obvious to an observer. Incorporating information about dimensions and determining the correlation between measurements of different dimensions (if any) would only add to the understanding of how the given building was constructed.

If a reliable correlation is found between dimensions, then the true measurement

of applicable now-lost dimensions could be modeled. Because lost dimensions are essentially censored observations, analysis of the originally excluded data falls into the survival analysis branch of statistics and is a missing data problem. An 'event' in this application is a break of one of the major dimensions. Instead of looking at time to event, however, interest is in the length of a given measurement. Survival analysis approaches could be used to determine which dimensions are more likely to break and at what rate.

Another potential method, related to Broadbent's method of minimizing the MSE of the simple equation (1) is to minimize the sum of squared errors (SSE). If equation (1) is treated as a linear regression problem, we have the equation $E(Y_i) = qM_i$ with two unknowns: q and M_i. This method differs from a standard linear regression problem because we are trying to determine the values of M_i, assuming q is known. This peculiarity is analogous to having a regression equation $Y_i = \beta_0 + \beta_1 X_i + \varepsilon_i$, $i = 1, 2, \ldots, n$ where β_1 is known, and we are trying to find the values of the independent variables X_i. If we generate M_i's for a range of q, we can build a regression model to estimate q. The optimal quantum is the value of $\hat{q}$ that minimizes the residuals.

The motivating principle of this project was to evaluate the efficacy of a value-neutral approach to determining units of measure in ancient Greek architecture (Pakkanen, 2004a). Whereas archaeologists search for quanta by inductive reasoning, this statistical method is based in deductive reasoning. In general, archaeological investigation of a quantum has involved the identification of a quantum in one of two ways: by attempting to fit a hypothetical quantum (for example, an established ancient foot-unit) against the measurement of building components, or by finding a quantum based on a fraction of an average building component, such as triglyph length. The second method is certainly preferred over the first. However, the cosine quantogram minimizes bias toward any particular value by finding a value that has

the greatest likelihood of being the true quantum when taking into account all measurements, not a suggestive few. Nonetheless, refinement of the methods is needed to achieve statistically significant results that are also architecturally and archaeologically reasonable.

A Appendix: SAS Program for the Cosine Quantogram Method

```
libname sgg '<path>';

*****************************************************************
Monte Carlo Simulations
*****************************************************************;
/* Sample WITH replacement 10000 times */
proc sort data=sgg.measurements;
   by building type;
run;

proc surveyselect data=sgg.measurements
   out=resample
   rate=1
   rep=10000
   method=urs
   seed=315709091
   outhits;

   strata building type;
run;

/* Concatenate original sample with MC samples and unround*/
data unrounded;
   set sgg.measurements resample;
   Y_unrnd = Y + ((0.5*(10**-decimal))*(2*ranuni(1324601)-1));
   keep ID building type dimension replicate Y_unrnd;
run;

*****************************************************************
Calculate the Cosine Quantogram 1x10^-3 precision)
*****************************************************************;
data cosineq_001;
   set unrounded;
   array Q Q1-Q584;
   array cosine cosine1-cosine584;
   start = 0.013;
```

```
   do over Q;
      Q = start + (_I_ - 1)*0.001;
      tau = 1/Q;
      cosine = cos(2 * arcos(-1) * Y_unrnd * tau);
   end;
   drop tau Q1-Q584;
run;

*****************************************************************
Find the optimum quantum for each subset of the data
   Q_...: all buildings and types grouped
   Q_b..: each building
   Q_1t.: each type for building 1
   Q_2t.: each type for building 2
*****************************************************************;
/* Q_... */
proc sort data=cosineq_001;
   by replicate;
run;
proc univariate data=cosineq_001 noprint;
   var cosine1-cosine584;
   by replicate;
   output out=phi_all sum=phi1-phi584;
run;

data Q_all;
   set phi_all;
   cos_max=max(of phi1-phi584);
   array Q Q1-Q584;
   array phi phi1-phi584;
   start = 0.013;
   do over Q;
      Q = start + (_I_ - 1)*0.001;
      if cos_max = phi then Q_star=Q;
   end;

   drop start cos_max Q1-Q584 phi1-phi584;
run;

proc sort data=unrounded;
   by replicate;
run;
```

```
proc sort data=Q_all;
   by replicate;
run;
data error_all;
   merge unrounded Q_all;
   by replicate;
   error = modz(Y_unrnd, Q_star);
   tau_star = 1/Q_star;
   if error > Q_star/2  then  error = error - Q_star;
   summand_all = cos(2* arcos(-1) * error * tau_star);

   drop tau_star;
run;

/* Q_b.. */
proc sort data=cosineq_001;
   by replicate building;
run;
proc univariate data=cosineq_001 noprint;
   by replicate building;
   var cosine1-cosine584;
   output out=phi_b sum=phi1-phi584;
run;
data Q_b;
   set phi_b;
   cos_max=max(of phi1-phi584);
   array Q Q1-Q584;
   array phi phi1-phi584;
   start = 0.013;
   do over Q;
      Q = start + (_I_ - 1)*0.001;
      if cos_max = phi then Q_star = Q;
   end;

   drop start cos_max Q1-Q584 phi1-phi584;
run;

proc sort data=unrounded;
   by replicate building;
run;
proc sort data=Q_b;
   by replicate building;
```

```
run;
data error_b;
   merge unrounded Q_b;
   by replicate building;
   error = modz(Y_unrnd, Q_star);
   tau_star = 1/Q_star;
   if error > Q_star/2  then  error = error - Q_star;
   summand_b = cos(2* arcos(-1) * error * tau_star);

   drop tau_star;
run;

/* Q_1t. */
proc sort data=cosineq_001;
   by replicate building type;
run;
proc univariate data=cosineq_001 noprint;
   by replicate building type;
   var cosine1-cosine584;
   output out=phi_t sum=phi1-phi584;
run;
data Q_1t;
   set phi_t;
   where building = 1;
   cos_max=max(of phi1-phi584);
   array Q Q1-Q584;
   array phi phi1-phi584;
   start = 0.013;
   do over Q;
      Q = start + (_I_ - 1)*0.001;
      if cos_max = phi then Q_star = Q;
   end;

   drop start cos_max Q1-Q584 phi1-phi584;
run;

proc sort data=unrounded;
   by replicate building type;
run;
proc sort data=Q_1t;
   by replicate building type;
run;
```

```
data error_1t;
   merge unrounded Q_1t;
   by replicate building type;
   where building = 1;
   error = modz(Y_unrnd, Q_star);
   tau_star = 1/Q_star;
   if error > Q_star/2  then  error = error - Q_star;
   summand_1t = cos(2* arcos(-1) * error * tau_star);

   drop tau_star;
run;

/* Q_2t. */
data Q_2t;
   set phi_t;
   where building = 2;
   cos_max=max(of phi1-phi584);
   array Q Q1-Q584;
   array phi phi1-phi584;
   start = 0.013;
   do over Q;
      Q = start + (_I_ - 1)*0.001;
      if cos_max = phi then Q_star = Q;
   end;

   drop start cos_max Q1-Q584 phi1-phi584;
run;

proc sort data=unrounded;
   by replicate building type;
run;
proc sort data=Q_1t;
   by replicate building type;
run;
data error_2t;
   merge unrounded Q_2t;
   by replicate building type;
   where building = 2;
   error = modz(Y_unrnd, Q_star);
   tau_star = 1/Q_star;
   if error > Q_star/2  then  error = error - Q_star;
   summand_2t = cos(2* arcos(-1) * error * tau_star);
```

```
   drop tau_star;
run;

/* Create a dataset with only the quanta from the original sample */
data sgg.quanta3;
   set Q_all Q_b Q_1t Q_2t;
   where replicate = 0;
   keep ID building type Q_star;
run;

*****************************************************************
Calculate Portions of Log-likelihood Ratios
*****************************************************************;
/* LLR_... */
proc univariate data=error_all noprint;
   by replicate;
   var summand_all;
   output out=stat_all sum=LLR_all;
run;

/* LLR_b.. */
proc univariate data=error_b noprint;
   by replicate;
   var summand_b;
   output out=stat_b sum=LLR_b;
run;

/* LLR_1.. */
proc univariate data=error_b noprint;
   where building = 1;
   by replicate;
   var summand_b;
   output out=stat_1 sum=LLR_1;
run;
/* LLR_2.. */
proc univariate data=error_b noprint;
   where building = 2;
   by replicate;
   var summand_b;
   output out=stat_2 sum=LLR_2;
run;
```

```
/* LLR_1t. */
proc univariate data=error_1t noprint;
   by replicate;
   var summand_1t;
   output out=stat_1t sum=LLR_1t;
run;
/* LLR_2t. */
proc univariate data=error_2t noprint;
   by replicate;
   var summand_2t;
   output out=stat_2t sum=LLR_2t;
run;

*****************************************************************
Calculate Log-likelihood Ratios
*****************************************************************;
/* Test #1: all buildings the same */
data test1;
   merge stat_all stat_b;
   by replicate;
   test_stat = LLR_all - LLR_b;
run;

data resampled1;
   set test1;
   if replicate = 0 then delete;
run;

/* Test #2: all types in building 1 are the same */
data test2;
   merge stat_1 stat_1t;
   by replicate;
   test_stat = LLR_1 - LLR_1t;
run;

data resampled2;
   set test2;
   if replicate = 0 then delete;
run;

/* Test #3: all types in building 2 are the same */
```

```
data test3;
   merge stat_2 stat_2t;
   by replicate;
   test_stat = LLR_2 - LLR_2t;
run;

data resampled3;
   set test3;
   if replicate = 0 then delete;
run;

data sgg.LLR;
   set test1 test2 test3;
   where replicate=0;
   keep test_stat;
run;
proc print data=sgg.LLR;
run;

*****************************************************************
Calculate Test Region
   Calculate percentiles (0 to 100 by 0.5)
   Find where the calculated LLR falls in the resampled LLRs
*****************************************************************;
/* Test #1: all buildings the same */
proc univariate data=resampled1 noprint;
   var test_stat;
   output out=LLR1 pctlpre=P_ pctlpts= 0 to 100 by 0.5;
run;
/* Test #2: all types in building 1 are the same  */
proc univariate data=resampled2 noprint;
   var test_stat;
   output out=LLR2 pctlpre=P_ pctlpts= 0 to 100 by 0.5;
run;
/* Test #3: all types in building 2 are the same  */
proc univariate data=resampled3 noprint;
   var test_stat;
   output out=LLR3 pctlpre=P_ pctlpts= 0 to 100 by 0.5;
run;
data sgg.test_region;
   set LLR1 LLR2 LLR3;
run;
```

```
proc print data=sgg.test_region;
run;

*****************************************************************
Calculate 95% Confidence Intervals
*****************************************************************;
data quanta_all;
   set Q_all;
   if replicate = 0 then delete;
run;
proc univariate data=quanta_all noprint;
   var Q_star;
   output out=stats_all pctlpre=P_ pctlpts=2.5, 97.5 std=SE;
run;
data stats_all;
   set stats_all;
   building = .;
   type = .;
run;

data quanta_b;
   set Q_b;
   if replicate = 0 then delete;
run;
proc sort data=quanta_b;
   by building;
run;
proc univariate data=quanta_b noprint;
   var Q_star;
   by building;
   output out=stats_b pctlpre=P_ pctlpts=2.5, 97.5 std=SE;
run;

data quanta_1t;
   set Q_1t;
   if replicate = 0 then delete;
run;
proc sort data=quanta_1t;
   by type;
run;
proc univariate data=quanta_1t noprint;
   var Q_star;
```

```
   by type;
   output out=stats_1t pctlpre=P_ pctlpts=2.5, 97.5 std=SE;
run;
data stats_1t;
   set stats_1t;
   building = 1;
run;

data quanta_2t;
   set Q_2t;
   if replicate = 0 then delete;
run;
proc sort data=quanta_2t;
   by type;
run;
proc univariate data=quanta_2t noprint;
   var Q_star;
   by type;
   output out=stats_2t pctlpre=P_ pctlpts=2.5, 97.5 std=SE;
run;
data stats_2t;
   set stats_2t;
   building = 2;
run;

proc sort data=sgg.quanta3;
   by building type;
run;
data sgg.summary;
   retain building type Q_star SE P_2_5 P_97_5;
   set stats_all stats_b stats_1t stats_2t;
   merge sgg.quanta3;
   by building type;
run;
proc print data=sgg.summary;
run;
```

References

Agostinelli, C., & Lund, U. (2007). *circular: Circular statistics.* Universitá Ca' Foscari Venezia.

Ashburner, J., & Friston, K. J. (2000). Voxel-based morphometry - The methods. *NeuroImage*, *11*, 805–821.

Aston, F. W. (1920). Isotopes and atomic weights. *Nature*, *105*(2646), 617–619.

Bankel, H. (1984). Moduli an den Tempeln von Tegea und Stratos? Grenzen der Fussmassbestimmung. *Archäologischer Anzeiger*, 409–430.

Baxter, M. (2003). *Statistics in archaeology.* London: Hodder Arnold.

Broadbent, S. R. (1955). Quantum hypotheses. *Biometrika*, *42*(1/2), 45–57.

Broadbent, S. R. (1956). Examination of a quantum hypothesis based on a single set of data. *Biometrika*, *43*(1/2), 32–44.

Chippendale, C. (1986). Archaeology, design theory, and the reconstruction of pre-historic design systems. *Environment and Planning B: Planning and Design*, *13*(4), 445–485.

Coulton, J. J. (1977). *Ancient Greek architects at work.* Ithaca, New York: Cornell University Press.

Courby, F., & Picard, C. (1924). *Recherches archéologiques à Stratos d'Acarnanie.* Paris.

Csörgő, S. (1980). On the quantogram of Kendall and Kent. *Journal of Applied Probability*, *17*(2), 440–447.

Dinsmoor, W. B. (1961). The basis of Greek temple design: Asia Minor, Greece, Italy. In *Atti del settimo congresso internazionale di archeologia* (Vol. 1, pp. 355–368). Rome: L'Erma di Bretschneider.

Freeman, P. R. (1976). A Bayesian analysis of the Megalithic yard. *Journal of the*

Royal Statistical Society. Series A (General), *139*(1), 20–55.

Hewson, A. D. (1980). The Ashanti weights - A statistical evaluation. *Journal of Archaeological Science*, *7*(4), 363–370.

Jammalamadaka, S. R., & SenGupta, A. (2001). *Topics in circular statistics*. River Edge, NJ: World Scientific.

Janson, H. W., & Janson, A. F. (2001). *History of art* (6th ed.). Upper Saddle River, NJ: Prentice Hall.

Kendall, D. G. (1974). Hunting quanta. *Philosophical Transactions of the Royal Statistical Society of London. Series A, Mathematical and Physical Sciences*, *276*(1257), 231–266.

Kent, J. T. (1975). A weak convergence theorem for the empirical characteristic function. *Journal of Applied Probability*, *12*(3), 515–523.

Koenigs, W. (1979). Zum Entwurf dorischer Hallen. *Istanbuler Mitteilungen*, *29*, 209–238.

Lehmann, K. (1998). *Samothrace: A guide to the excavations and the museum* (6th rev. ed.). Thessaloniki: Institute of Fine Arts, New York University Press.

Lehmann, P. W. (1969a). *Samothrace. Excavations conducted by the Institute of Fine Arts, New York University* (Vol. 3: The Hieron (Plates)). Princeton: Princeton University Press.

Lehmann, P. W. (1969b). *Samothrace. Excavations conducted by the Institute of Fine Arts, New York University* (Vol. 3: The Hieron (Text I)). Princeton: Princeton University Press.

Lockhart, R. A., & Stephens, M. A. (1985). Tests of fit for the von Mises distribution. *Biometrika*, *72*(3), 647–652.

Manly, B. F. J. (2007). *Randomization, bootstrap and Monte Carlo methods in biology* (3rd ed.). Boca Raton: Chapman and Hall/CRC.

Mardia, K. V., & Jupp, P. E. (2000). *Directional statistics* (2nd ed.). Chichester: John Wiley and Sons.

Marriott, F. H. C. (1979). Barnard's Monte Carlo tests: How many simulations? *Applied Statistics*, *28*(1), 75–77.

Matsas, D., & Bakirtzis, A. (2001). *Samothrace: A short cultural guide* (2nd ed.). Municipality of Samothrace.

Mertens, D. (1984). *Der Tempel von Segesta und die dorische Tempelbaukunst des griechischen Westens in klassicher Zeit*. Mainz: Philipp von Zabern.

Newson, R. B., Parker, J. S., & Barlow, P. W. (1993). Are lateral roots of tomato spaced by multiples of a fundamental distance? *Annals of Botany*, *71*, 549–557.

Pakkanen, J. (2002). Deriving ancient foot units from building dimensions: A statistical approach employing cosine quantogram analysis. In G. Burenhult & J. Arvidsson (Eds.), *Archaeological informatics: Pushing the envelope - CAA 2001 - Computer applications and quantitative methods in archaeology, Proceedings of the 29th conference, Gotland, April 2001, BAR* (Vol. 1016, pp. 501–505). Oxford: Archaeopress.

Pakkanen, J. (2004a). The Temple of Zeus at Stratos: New observations on the building design. *Arctos*, *38*, 95–121.

Pakkanen, J. (2004b). The Toumba building at Lefkandi: A statistical method for detecting a design-unit. *The Annual of the British School at Athens*, *99*, 258–271.

Pakkanen, J. (2005). The Temple of Athena Alea at Tegea: Revisiting design-unit derivation from building measurements. In E. Østby (Ed.), *Ancient Arcadia. Third international seminar on ancient arcadia, Held at the Norwegian Institute at Athens, 7-10 May 2002* (p. 167-183). Athens: Norwegian Institute at Athens.

Prout, W. (1815). On the relation between the specific gravities of bodies in their

gaseous state and the weights of their atoms. *Annals of Philosophy*, *6*, 321–330.

Rottländer, R. C. A. (1996). New ideas about old units of length. *Interdisciplinary Science Reviews*, *21*(3), 235–242.

Thaler, H. T., & Braun, H. I. (1984). On the apparent clustering of clonal albumin production and enzyme activity levels. *Biometrics*, *40*(4), 1095–1102.

Thom, A. (1955). A statistical examination of the Megalithic sites in Britain. *Journal of the Royal Statistical Society. Series A (General)*, *118*(3), 275–295.

Upton, G. J. G. (1973). Single-sample tests for the von Mises distribution. *Biometrika*, *60*(1), 87–99.

Von Mises, R. (1918). Über die 'Ganzzahligkeit' der Atomgewichte und verwandte Fragen. *Physikalische Zeitschrift*, *19*, 490–500.

Watson, G. S. (1961). Goodness-of-fit tests on a circle. *Biometrika*, *48*, 109–114.

Wescoat, B. (forthcoming). *Samothrace. Excavations conducted by the Institute of Fine Arts, New York University* (Vol. 9: Monuments of the Eastern Hill). (Manuscript submitted for publication)

Wilson Jones, M. (2000). Doric measure and architectural design 1: The evidence of the relief from Salamis. *American Journal of Archaeology*, *104*(1), 73–93.

Wilson Jones, M. (2001). Doric measure and architectural design 2: A modular reading of the classical temple. *American Journal of Archaeology*, *105*(4), 675-713.